© 2020. Published by The Company of Biologists Ltd | Development (2020) 147, dev187013. doi:10.1242/dev.187013

HUMAN DEVELOPMENT

RESEARCH ARTICLE

Cytotrophoblast extracellular vesicles enhance decidual cell secretion of immune modulators via TNFα

Sara K. Taylor[1,2,3], Sahar Houshdaran[1,2], Joshua F. Robinson[1,2,3], Matthew J. Gormley[1,2,3], Elaine Y. Kwan[2], Mirhan Kapidzic[1,2,3], Birgit Schilling[4], Linda C. Giudice[1,2] and Susan J. Fisher[1,2,3,5,6,7,*]

ABSTRACT

The placenta releases large quantities of extracellular vesicles (EVs) that likely facilitate communication between the embryo/fetus and the mother. We isolated EVs from second trimester human cytotrophoblasts (CTBs) by differential ultracentrifugation and characterized them using transmission electron microscopy, immunoblotting and mass spectrometry. The 100,000 ***g*** pellet was enriched for vesicles with a cup-like morphology typical of exosomes. They expressed markers specific to this vesicle type, CD9 and HRS, and the trophoblast proteins placental alkaline phosphatase and HLA-G. Global profiling by mass spectrometry showed that placental EVs were enriched for proteins that function in transport and viral processes. A cytokine array revealed that the CTB 100,000 ***g*** pellet contained a significant amount of tumor necrosis factor α (TNFα). CTB EVs increased decidual stromal cell (dESF) transcription and secretion of NF-κB targets, including IL8, as measured by qRT-PCR and cytokine array. A soluble form of the TNFα receptor inhibited the ability of CTB 100,000 ***g*** EVs to increase dESF secretion of IL8. Overall, the data suggest that CTB EVs enhance decidual cell release of inflammatory cytokines, which we theorize is an important component of successful pregnancy.

KEY WORDS: Human, Placenta, Cytotrophoblast, Extracellular vesicle, TNFα, Decidua

INTRODUCTION

Pregnancy presents unique physiologic and immunologic challenges to the mother and the embryo/fetus. The placenta mediates their physiologic integration. At a molecular level, this is accomplished by diverse molecules, including hormones and specialized placental proteins. At an immunologic level, the molecules and mechanisms are less clear, but likely include numerous chemokines and cytokines produced at the maternal-fetal interface and the cytotrophoblast MHC class I molecule HLA-G (Ellis et al., 1986; Hemberger, 2013; Kovats et al., 1990).

[1]Center for Reproductive Sciences, University of California, San Francisco, CA 94143, USA. [2]Department of Obstetrics, Gynecology, and Reproductive Sciences, University of California, San Francisco, CA 94143, USA. [3]Eli and Edythe Broad Center for Regeneration Medicine and Stem Cell Research, University of California, San Francisco, CA 94143, USA. [4]Chemistry & Mass Spectrometry, Buck Institute for Research on Aging, Novato, CA 94945, USA. [5]Division of Maternal Fetal Medicine, University of California, San Francisco, CA 94143, USA. [6]Department of Anatomy, University of California, San Francisco, CA 94143, USA. [7]Human Embryonic Stem Cell Program, University of California, San Francisco, CA 94143, USA.

*Author for correspondence (susan.fisher@ucsf.edu)

S.K.T., 0000-0002-4086-3471; S.H., 0000-0003-3163-5298; J.F.R., 0000-0002-2421-4535; M.J.G., 0000-0003-2042-1534; E.Y.K., 0000-0002-5113-3044; M.K., 0000-0001-9723-402X; B.S., 0000-0001-9907-2749; L.C.G., 0000-0002-1677-0822; S.J.F., 0000-0001-7745-4850

Handling Editor: Liz Robertson
Received 22 April 2020; Accepted 23 July 2020

The placenta also mediates the physical integration of the embryo/fetus with the uterus and the maternal circulatory system. Its functional units are termed chorionic villi, which are classified as either floating or anchoring (Robinson et al., 2017). Most of the placental surface is composed of floating villi, which are suspended in maternal blood (Maltepe and Fisher, 2015). Their surface is formed by syncytiotrophoblasts (STBs) – multinucleated cells covered in microvilli, which increase the surface area and consequently diffusion, promoting nutrient and waste exchange (Smith et al., 1977). Beneath the STB layer lie progenitor mononuclear cytotrophoblasts (CTBs), which fuse to form the syncytium (Robinson et al., 2017). The stromal core lies deep to the CTB layer and contains the villous vascular tree and connective tissue elements, including a specialized population of macrophages (Hoffbauer cells) (Gaw et al., 2019; Red-Horse et al., 2005). In anchoring villi, the CTB progenitors aggregate into columns that leave the placenta and invade the decidua, where they remodel spiral arteries, redirecting blood flow to the floating villi (Red-Horse et al., 2005). The commingling of placental cells from the embryo/fetus and maternal immune, decidual and muscle cells within the uterus requires fine tuning tolerizing and inflammatory mechanisms (Hemberger, 2013).

The placenta produces large numbers of extracellular vesicles (EVs) that increase in concentration throughout gestation (Germain et al., 2007; Knight et al., 1998; Salomon et al., 2014; Sarker et al., 2014). EVs are an emerging form of intercellular communication (Kalluri and LeBleu, 2020). Functions of these vesicles have been most intensively studied in the context of cancer, in which they promote angiogenesis, metastasis, remodeling of the pre-metastatic niche at distal sites, and immune suppression (Costa-Silva et al., 2015; Hoshino et al., 2015; Huang and Feng, 2017; Peinado et al., 2012; Poggio et al., 2019). The component processes of human placentation have many parallels with tumorigenesis and metastasis. CTBs invade the uterus, breach the vasculature and modulate the maternal immune system to promote tolerance of the feto-placental unit (Hemberger, 2013; Maltepe and Fisher, 2015). This implies that placental EVs might have functions in common with those produced by cancer cells.

Initial studies of placental EVs focused on the subset generated by STBs (reviewed by Tannetta et al., 2017). Fewer studies have explored the functions of EVs produced by primary CTBs. In general, they too have immunomodulatory roles. For example, term CTB exosomes confer viral resistance to recipient non-placental cells, including human umbilical vein endothelial cells (HUVECs), human uterine microvascular endothelial cells (HUtMVECs), placental fibroblasts and foreskin fibroblasts (Delorme-Axford et al., 2013; Ouyang et al., 2016). This activity was attributed to miRNAs from the placenta-specific chromosome 19 cluster (C19MC) that are found in trophoblasts and their vesicles (Donker et al., 2012). Transfection of this cluster into recipient

Development (2020) 147, dev187013. doi:10.1242/dev.187013

cells also attenuates viral replication (Delorme-Axford et al., 2013). In addition, primary term villous CTB 100,000 ***g*** EVs suppress secretion of Th1 cytokines – IL2, TNFα, and IFNγ – in activated Jurkat T cells and peripheral blood mononuclear cells (PBMCs); this activity is blocked by inhibition of syncytin-2 (also known as ERVFRD-1) (Lokossou et al., 2019). The function of CTB EVs at mid-gestation has not been studied.

Here, we describe the size, morphology and protein contents of two types of second trimester CTB EVs. We profiled their proteome using a targeted immunoblot approach and more globally by mass-spectrometry. Through a cytokine array, we identified significant levels of TNFα in the 100,000 ***g*** EVs. As CTB-conditioned medium amplifies decidual stromal cell expression and secretion of NF-κB target pro-angiogenic cytokines (Hess et al., 2007), we investigated the role of CTB 100,000 ***g*** EVs and TNFα in this context.

RESULTS

CTBs produced extracellular vesicles that contained exosomal and placental markers

We isolated two populations of EVs from the conditioned medium of second trimester CTBs by ultracentrifugation. As the source was primary cells, the limited amount of material precluded additional purification steps, such as density gradient centrifugation and/or immunoaffinity isolation. We expected the 16,500 ***g*** EV pellet to be enriched for microvesicles and the 100,000 ***g*** EV pellet to be enriched for exosomes. Transmission electron microscopy (TEM) of grid areas with high concentrations of vesicles revealed that the lower speed pellet was comprised of a heterogeneous population that included larger, crenulated structures and smaller exosome-like EVs (Fig. 1A). The majority (61%) were less than 150 nm (Fig. 1B). In contrast, the higher speed pellet was enriched for vesicles with a cup-like morphology typical of exosomes (Fig. 1C). The majority of these EVs were smaller in size; 86% were less than 150 nm (Fig. 1D). As microvesicles and exosomes overlap in size, this heterogeneity was expected for EVs isolated by ultracentrifugation.

Initially, we used immunoblotting methods to compare the protein contents of 16,500 ***g*** and 100,000 ***g*** EVs to CTB lysates. The results are shown in Fig. 2. Representative immunoblots (upper panels) are paired with densitometry analyses, in which the relative intensity of bands was normalized to the 100,000 ***g*** lane (lower panels). With regard to exosomal markers, tetraspanin (CD9) was only detected in the 100,000 ***g*** EVs (Fig. 2A), which also contained the ESCRT-0 component HRS (HGS) (Fig. 2B). These results were consistent with the TEM, reinforcing the conclusion that the 100,000 ***g*** pellet was enriched for exosomes and the 16,500 ***g*** pellet was a heterogeneous population that also contained these vesicles.

With regard to placenta-specific markers, we were interested in whether these EVs contained the human trophoblast-specific nonclassical MHC class I molecule HLA-G (Kovats et al., 1990; McMaster et al., 1995). As expected, the monomer, which appeared as a diffuse band owing to complex glycosylation, was the major form associated with CTB lysates (Fig. 2C) (McMaster et al., 1998). The 16,500 ***g*** EVs contained both the monomer and dimer. In comparison, the 100,000 ***g*** EVs were significantly enriched for dimeric HLA-G. Importantly, this form of the molecule has a higher affinity for its receptors, LILRB1 and LILRB2, suggesting enhancement of inhibitory signals (Kuroki et al., 2019; Shiroishi et al., 2006). Placental alkaline phosphatase (PLAP; ALPP) had a similar expression pattern in both EV fractions, with the highest relative abundance in the 100,000 ***g*** EVs (Fig. 2D).

We immunoblotted for other molecules, the functions of which in exosomes are relevant to the biology of pregnancy. Placental EVs contained the adhesion-promoting extracellular matrix (ECM) molecule fibronectin (FN; Fig. 2E), the expression of which was strikingly higher in 100,000 ***g*** EVs compared with the 16,500 ***g*** fraction. PDL1 (CD274), a suppressor of T cell activation (Poggio et al., 2019), was detected in CTB lysates and both populations of vesicles (Fig. 2F), suggesting that these EVs could have immune inhibitory properties.

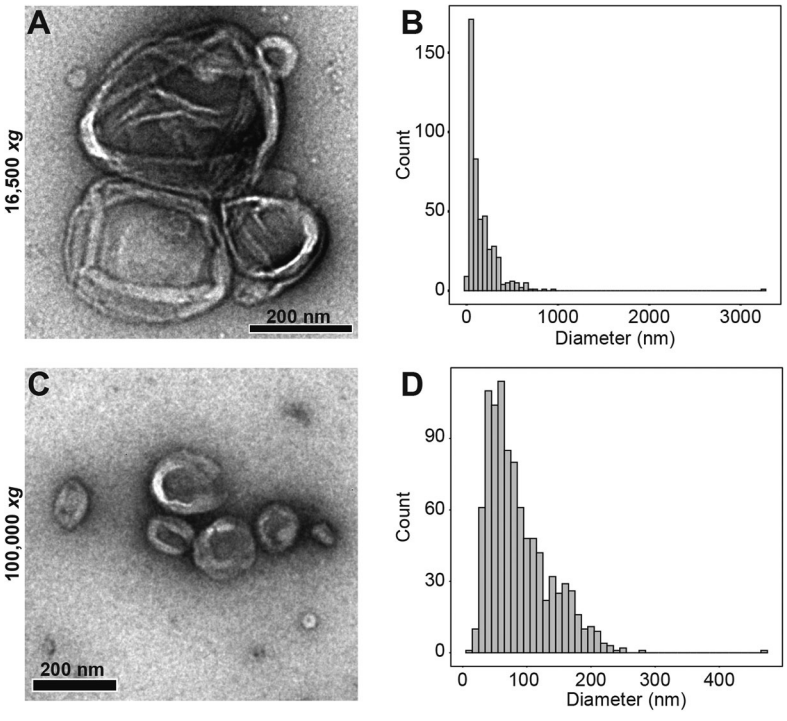

Fig. 1. CTB EVs analyzed by TEM displayed the expected morphology and size. (A) TEM of the 16,500 ***g*** fraction demonstrated that they are a heterogeneous population that included larger crenulated vesicles and smaller exosome-like EVs with a cup-like morphology. (B) A histogram of this fraction showed a range of sizes, with most vesicles (61%) less than 150 nm in diameter. (C) TEM revealed that the 100,000 ***g*** pellet was enriched for vesicles with a morphology typical of exosomes. (D) A histogram of this fraction showed that it was composed of mainly smaller EVs, with the majority (86%) less than 150 nm in diameter. *n*=3 biological replicates. Scale bars: 200 nm.

Development (2020) 147, dev187013. doi:10.1242/dev.187013

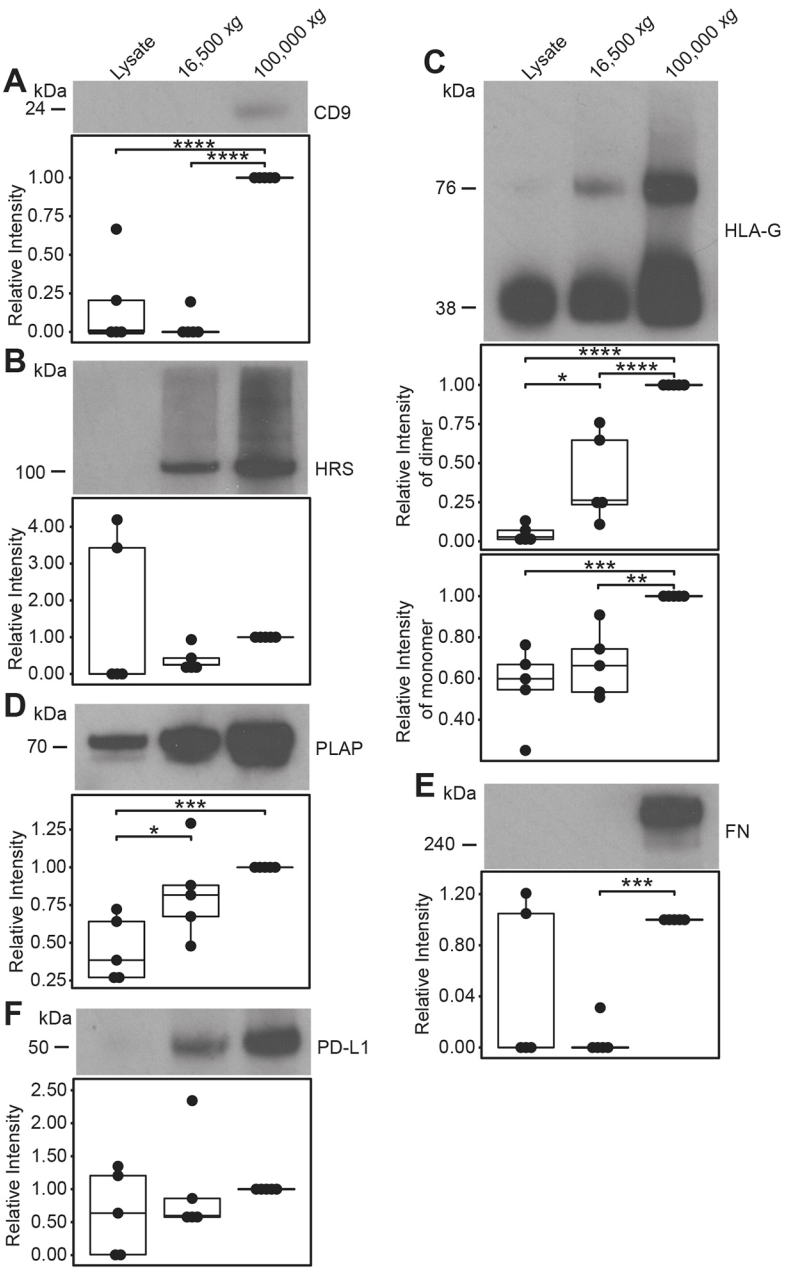

Fig. 2. CTB 100,000 *g* EVs were enriched for exosomal and placental markers. (A-F) Representative immunoblots comparing CTB lysate, 16,500 ***g*** EVs and 100,000 ***g*** EVs are displayed. Relative intensity was measured by densitometry. (A) The exosomal marker CD9 was only detected in the 100,000 ***g*** fraction. (B) Both EV pellets contained the ESCRT-0 component HRS. (C) CTB lysate primarily expressed monomeric HLA-G, an invasive CTB marker. The dimer was detected in the 16,500 ***g*** pellet, whereas the 100,000 ***g*** fraction was enriched for both forms of the molecule. (D) Placental marker PLAP was enriched in both EV fractions. (E) Fibronectin (FN) levels were variable in the cell lysate and only detected in the 100,000 ***g*** fraction. (F) Likewise, cell-associated levels of PDL1 varied, but were consistently detected in both EV pellets. *n*=5 biological replicates. **P*<0.05, ***P*<0.01, ****P*<0.005, *****P*<0.001 (one-way ANOVA with Dunnett's test).

Global proteomic analysis of CTB EVs

We performed mass spectrometry profiling of the protein contents of second trimester CTB EVs. We identified 811 proteins in 16,500 ***g*** EVs and 427 proteins in 100,000 ***g*** EVs (Fig. 3A, Tables S1 and S2). Of these, 377 were components of both vesicle types, 434 were unique to the 16,500 ***g*** fraction, and 50 were found only in the 100,000 ***g*** pellet. More proteins may have been identified in the 16,500 ***g*** samples owing to EV heterogeneity and/or the larger size of the component vesicles.

Multiple exosomal markers were detected in CTB EVs: CD9 and CD81 were identified in both vesicle types, whereas CD63, TSG101 and CD82 were only found in the 100,000 ***g*** fraction (Raposo and Stoorvogel, 2013). In both EV populations, we identified molecules with immune functions, including CD47, CD59, CD276, and galectin 3 (LGALS3). In addition, HLA-G was only detected in the 100,000 ***g*** pellet, reflecting the enrichment of this molecule that was observed by immunoblot (Fig. 2C). Both EV types contained multiple proteasome subunits, which process antigens for peptide presentation by class I MHC molecules (Vigneron et al., 2017), suggesting that this process might be occurring.

Proteins involved in iron transport, such as HLA-H, transferrin receptor protein 1 (TFRC) and serotransferrin (TF), were identified in both vesicle fractions (Garrick, 2011; Pascolo et al., 2005). We also detected proteins previously associated with placental EVs, such as the retrotransposon-derived protein PEG10, endoglin, DPPIV and trophoblast glycoprotein (Abed et al., 2019; Alam et al., 2018; Kandzija et al., 2019; Tannetta et al., 2013). Both vesicle types contained multiple CTB adhesion-related molecules: fibronectin; Eph family members; integrins α1, α5, α6, β1, and β4; and laminin subunits (Damsky and Fisher, 1998; Red-Horse et al., 2005). In other systems, these molecules are crucial for vesicles homing to target cells (Hoshino et al., 2015). We also detected components of prostaglandin pathways, including 15-hydroxyprostaglandin dehydrogenase, prostaglandin E synthase

Development (2020) 147, dev187013. doi:10.1242/dev.187013

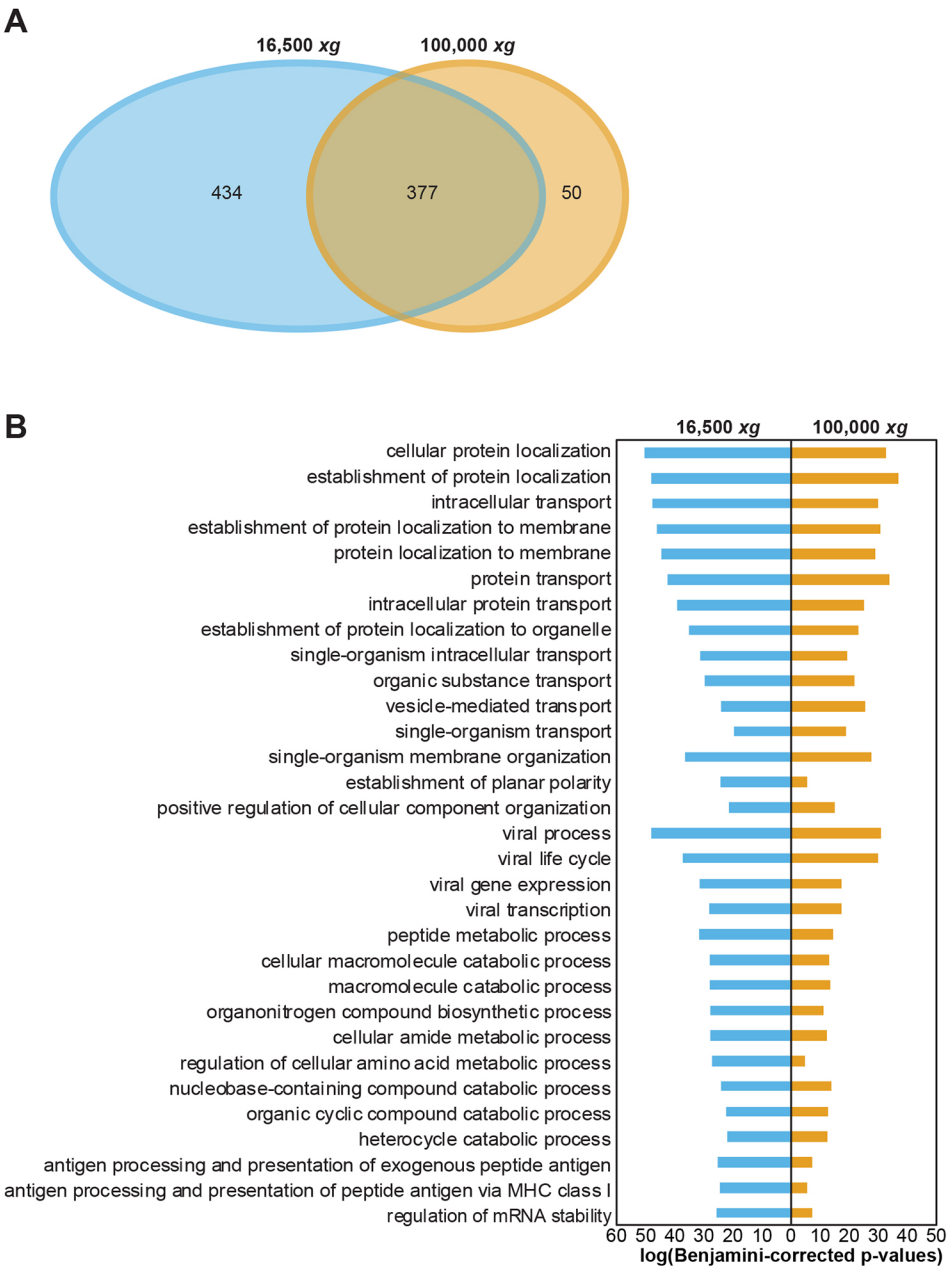

Fig. 3. Global profiling of CTB EVs revealed their protein contents. (A) Mass spectrometry profiling identified 811 proteins in CTB 16,500 ***g*** EVs and 427 proteins in CTB 100,000 ***g*** EVs. Of the identified proteins, 377 were shared between both populations, 434 were unique to the 16,500 ***g*** pellet, and 50 were only found in the 100,000 ***g*** fraction. (B) The proteome of each vesicle type was matched to GO terms. The most significant 25 biological processes for each EV type mainly fell into three categories: localization and transport, viral pathways and metabolism. Cellular organization, antigen processing/presentation and regulation of RNA stability were also represented. *n*=2.

3 and prostaglandin F2 receptor negative regulator. CTB EVs also contained proteins with cancer-related functions: neuroblast differentiation associated protein AHNAK, present in both vesicle populations, promotes tumor migration, invasion and EV release (Shankar et al., 2010; Silva et al., 2016), whereas glia-derived nexin, detected in the 100,000 ***g*** fraction, mediates tumor vascular mimicry (Wagenblast et al., 2015). Overall, the EV proteome contained an interesting protein repertoire with functions that are highly relevant to placental processes.

The proteome of each vesicle type was matched to Gene Ontology (GO) terms. Statistical significance was greater for 16,500 ***g*** pathways compared with that of 100,000 ***g***, likely because of the fact that the former contained approximately twice the number of proteins. The top biological processes that were represented by EV contents mainly fell into three categories: localization and transport, viral pathways, and metabolism (Fig. 3B). Viral processes were highlighted because of many proteins in these pathways with membrane budding functions. Cellular organization, vesicle-mediated transport, antigen processing and presentation, and regulation of RNA stability were also enriched. The number of highly related processes identified suggested that these could be important EV functions.

CTB 100,000 *g* EVs contained TNFα

Given that proteins with immune functions were a significant component of CTB EVs, we performed a cytokine array (Luminex High Sensitivity T Cell panel) to identify cargo that may be present at biologically active concentrations too low to be detected by mass spectrometry. In these experiments, we compared the contents of CTB 16,500 ***g*** and 100,000 ***g*** EVs. As a control for placenta-specific vesicle functions, we included 100,000 ***g*** EVs isolated from the K562 erythroleukemic cell line, an abundant source of vesicles (Rivoltini et al., 2016; Savina et al., 2002). Most analytes were below the threshold of detection, but low levels of IL6 (~0.2 pg/µg;

Development (2020) 147, dev187013. doi:10.1242/dev.187013

P<0.05) and MIP-3a (CCL20; ∼1 pg/µg; P<0.001) were detected in the 100,000 ***g*** EV fraction (Fig. S1). In contrast, relatively high levels of TNFα (∼5 pg/µg protein) were associated with these vesicles (P<0.001; Fig. 4A).

To confirm this finding, we examined CTB TNFα expression *in situ*. Immunolocalization at the maternal-fetal interface showed expression among cytokeratin-positive invasive CTBs (Fig. 4B,C). This staining was consistent with previously reported results (Phillips et al., 2001; Pijnenborg et al., 1998).

CTB EVs induced decidual cell transcription and secretion of cytokines

Our previous work showed that CTB-conditioned medium amplifies decidual cell expression and secretion of angiogenic and immune-modulating factors (Hess et al., 2007). Specifically, GO analysis suggested the mechanism involved activation of the NF-κB cascade. Given that fibroblast exosomal TNFα activates NF-κB signaling in target cells, including other fibroblasts and T cells (Zhang et al., 2006), we asked whether TNFα-containing CTB 100,000 ***g*** EVs induced expression and secretion of NF-κB targets in decidualized endometrial stromal fibroblasts (dESFs), the predominant cell in the decidua, over 24 h of culture (Fig. 5A). As in the cytokine analyses above, 100,000 ***g*** EVs from the K562 cell line were used as controls.

Changes in gene expression were measured using a chip-based qRT-PCR method (Fluidigm). Of the 40 analytes for which mRNAs were quantified, 12 genes were significantly upregulated by CTB 100,000 ***g*** EVs compared with PBS control, with the most significant changes at 3 h (Fig. 5B). They included *IL8* (*CXCL8*), *IL6*, *CXCL1* (*GRO1*), *CCL2* (*MCP-1*), *CSF1*, *ICAM1*, *NFKB1*, *NFKB2*, *RELB*, *TNFAIP2* and *TNFAIP3*, which are known targets of NF-κB activation, and *IRAK2* (Anisowicz et al., 1991; Brach et al., 1991; Bren et al., 2001; Hohensinner et al., 2007; Kang et al., 2007; Kunsch and Rosen, 1993; Libermann and Baltimore, 1990; Lombardi et al., 1995; Son et al., 2008; Ten et al., 1992; Ueda et al., 1994; van de Stolpe et al., 1994; Zhou et al., 2003). Previous work described above identified *IL8*, *IL6*, *CXCL1* and *CCL2* as among the genes most highly upregulated by CTB-conditioned medium (Hess et al., 2007); the data for these molecules are shown in Fig. 6, and the corresponding data for the remainder of the upregulated analytes are in Fig. S2. Compared with the PBS control, treatment with CTB 100,000 ***g*** EVs increased mRNA levels of *IL8* by 4.8-fold (Fig. 6A), *IL6* by 2.8-fold (Fig. 6B), *CXCL1* by 5.2-fold (Fig. 6C) and *CCL2* by 5.4-fold (Fig. 6D) at the 3 h time point. With the exception of *IL6*, CTB 16,500 ***g*** EV treatment increased mRNA levels of *LIF* and most NF-κB targets upregulated by the 100,000 ***g*** fraction at 3 h (Fig. 5B and Fig. S2). Compared with PBS controls, transcription returned to baseline levels at 12 h and 24 h. K562 100,000 ***g*** EVs did not significantly change mRNA levels of target genes compared with PBS controls (Fig. 5B).

We calculated that EVs in the above experiments contained ∼10 pg of TNFα based on the data shown in Fig. 4. To determine whether this cytokine alone could recapitulate the effects of CTB 100,000 ***g*** EVs, we treated dESFs with the recombinant version of this molecule [recombinant human TNFα (rhTNFα)] at an equivalent concentration and a 10-fold lower amount over the course of 24 h. A 10-fold higher concentration was omitted owing to obvious cell death. The transcriptional response was similar to that of CTB 100,000 ***g*** EV treatment, but upregulation of many target genes was sustained at each time point analyzed (Fig. S3). For example, we observed upregulation of *IL8*, *IL6*, *CXCL1* and *CCL2* (Fig. S4). Additional targets included: *JUNB*, *RELB*, *EGFR*, *LIF*, *IRAK2*, *ICAM1*, *NFKB2*, *TNFAIP3*, *CSF1* and *NFKB1* (Fig. S3). A few genes had different expression patterns. *TNFAIP2* was upregulated at 3 h and 24 h. Other genes (*RELA*, *IL7*, *FZD1*, *FZD2* and *JUN*) were modulated at only one time point. Overall, the number, magnitude and duration of transcriptional changes were greater in dESFs treated with an equivalent concentration of rhTNFα compared with CTB EVs, possibly because these vesicles contained other molecules that constrain the response to this cytokine.

We extended the CTB EV mRNA data to the protein level by performing another Luminex cytokine array for upregulated targets. Compared with PBS controls, CTB 100,000 ***g*** EVs increased dESF secretion of a number of chemokines/cytokines. However, the kinetics were different for each analyte. Levels of IL8 increased at 3 and 12 h (Fig. 7A). Similarly, CTB 100,000 ***g*** EVs increased CXCL1 secretion, particularly at 3 h (Fig. 7B). In contrast, their effects on CCL2 peaked at 12 h (Fig. 7C).

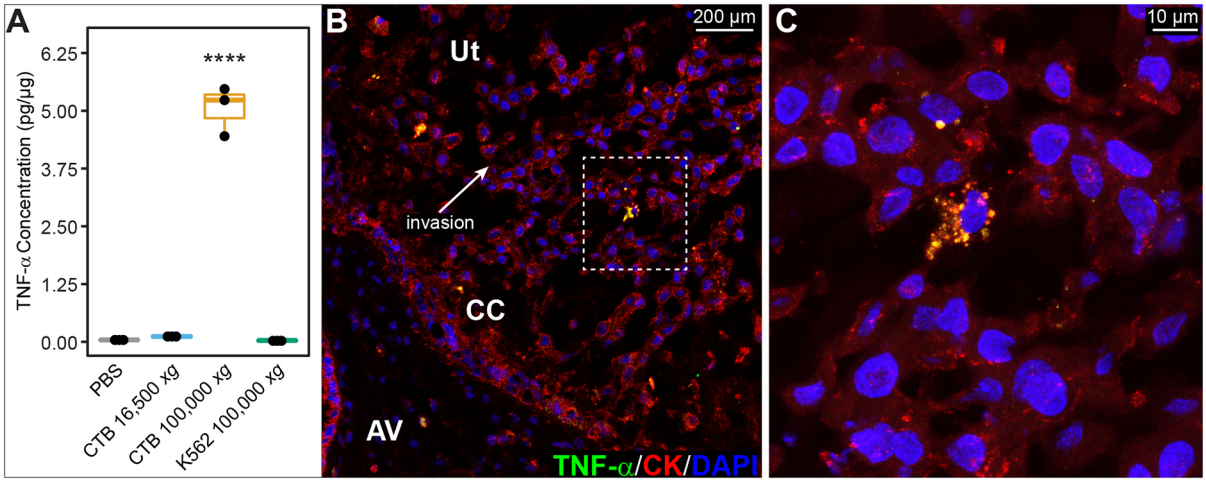

Fig. 4. TNFα was detected in association with CTB 100,000 *g* EVs produced *in vitro* and invasive CTBs *in situ*. (A) As measured by a high-sensitivity cytokine array, CTB 100,000 ***g*** EVs contained ∼5 pg TNFα per 1 µg total. n=3 biological replicates. ****P<0.001 (one-way ANOVA with Bonferroni correction). (B,C) Tissue sections of the basal plate were stained for the CTB marker cytokeratin (CK, red), TNFα (green) and DAPI (blue) and imaged at 20× (B) and 63× (C, magnification of boxed area in B). CK-positive CTBs immunostained for TNFα in a vesicular pattern. AV, anchoring villi; CC, cell column; Ut, uterus. n=3 biological replicates. Scale bars: 200 µm in B; 10 µm in C.

Development (2020) 147, dev187013. doi:10.1242/dev.187013

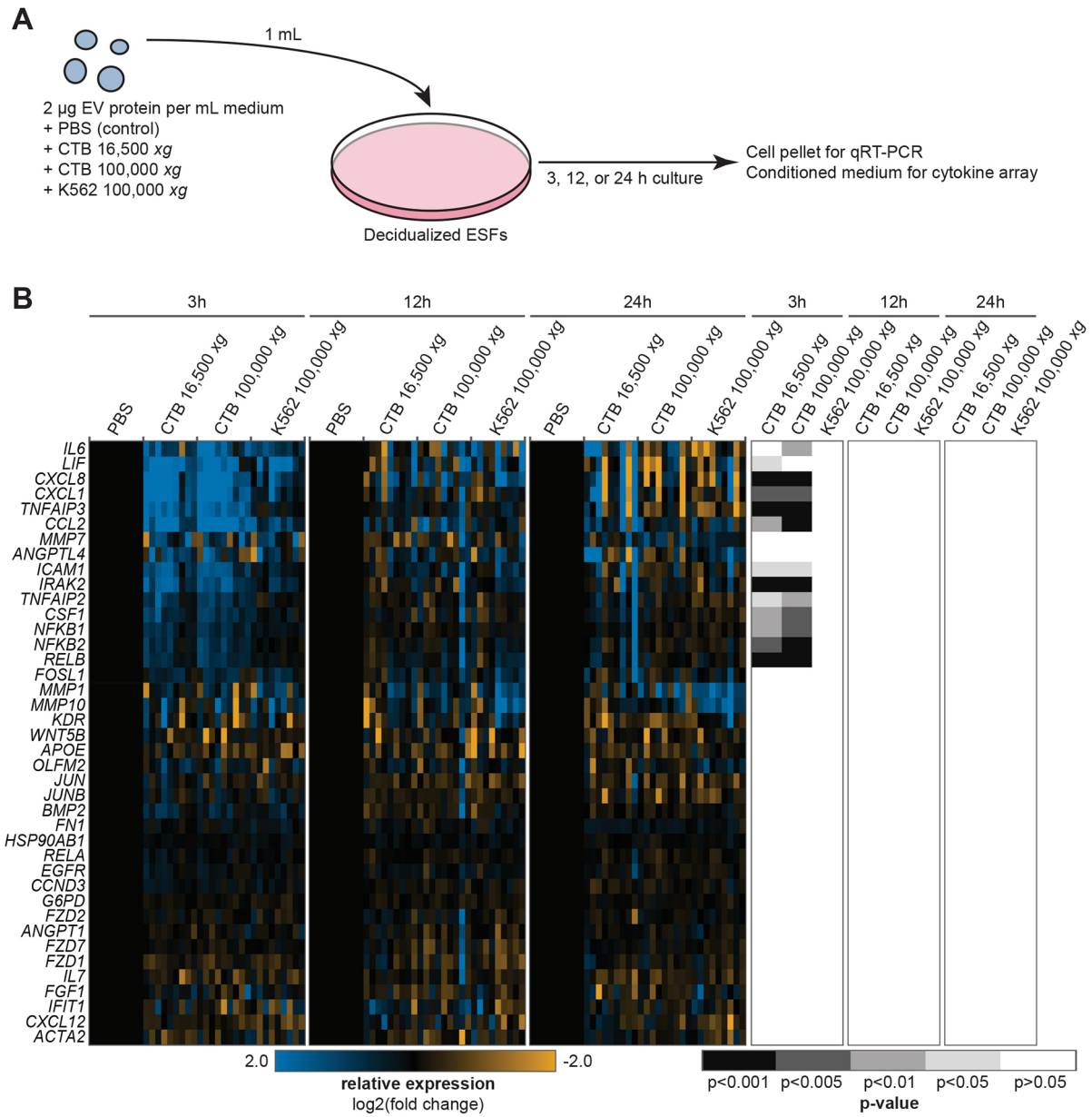

Fig. 5. CTB 100,000 *g* EVs increased expression of NF-κB targets (3 h) before returning to baseline (12 and 24 h). (A) Schematic of the *in vitro* assay used to determine the effects of CTB EVs on dESFs. Three sets of human primary dESFs were treated with three batches of CTB 16,500 ***g*** EVs, CTB 100,000 ***g*** EVs, K562 100,000 ***g*** EVs or PBS (control). EVs were added to dESF medium to a final concentration of 2 µg/ml and 1 ml was added to each tissue culture well. The cells were cultured for 3, 12 or 24 h. Then conditioned medium was collected for analysis by a cytokine array (Fig. 7) and cell pellets were harvested for qRT-PCR. (B) Heat maps of gene expression changes in dESFs as measured by a Fluidigm 96.96 Dynamic Array (left) and *P*-values compared with the PBS control (right). CTB EVs transiently increased transcription of NF-κB target genes at 3 h. *n*=3 biological replicates (EV batches and dESFs).

EV-induced IL6 secretion did not significantly change at any individual time point, but in the aggregate, the EVs had a significant positive effect (Fig. 7D). Likewise, a generalized linear model showed that CTB 100,000 ***g*** EVs increased dESF secretion of the other three factors shown in Fig. 7 over the 24 h course of the experiment ($P<0.001$).

Next, we asked whether the CTB 100,000 ***g*** EV effects on dESFs were unique. Compared with the PBS control, CTB 16,500 ***g*** EVs had a similar effect on dESF secretion of the chemokines/cytokines we analyzed. All four factors significantly increased over the course of the experiment as determined by a generalized linear model. However, the observed increases were smaller in magnitude (Fig. 7A-D). K562 100,000 ***g*** EVs did not significantly increase secretion of the four factors compared with the PBS control at any individual time point, but IL8 secretion was increased over the course of the experiment (Fig. 7A-D).

Finally, we asked whether the addition of rhTNFα at a concentration comparable with that of CTB 100,000 ***g*** EVs could mimic their effects at the protein level. Here, we focused on IL8, the dESF chemokine/cytokine with the most robust response to CTB EVs. The addition of rhTNFα at 1 and 10 pg/ml induced dESF secretion of IL8 at all time points analyzed in a dose-dependent manner as measured by ELISA (Fig. S5). This increase was much greater than the effects of CTB 100,000 ***g*** EV treatment, likely because the vesicles contain other immunomodulatory contents that may constrain the response to TNFα.

Development (2020) 147, dev187013. doi:10.1242/dev.187013

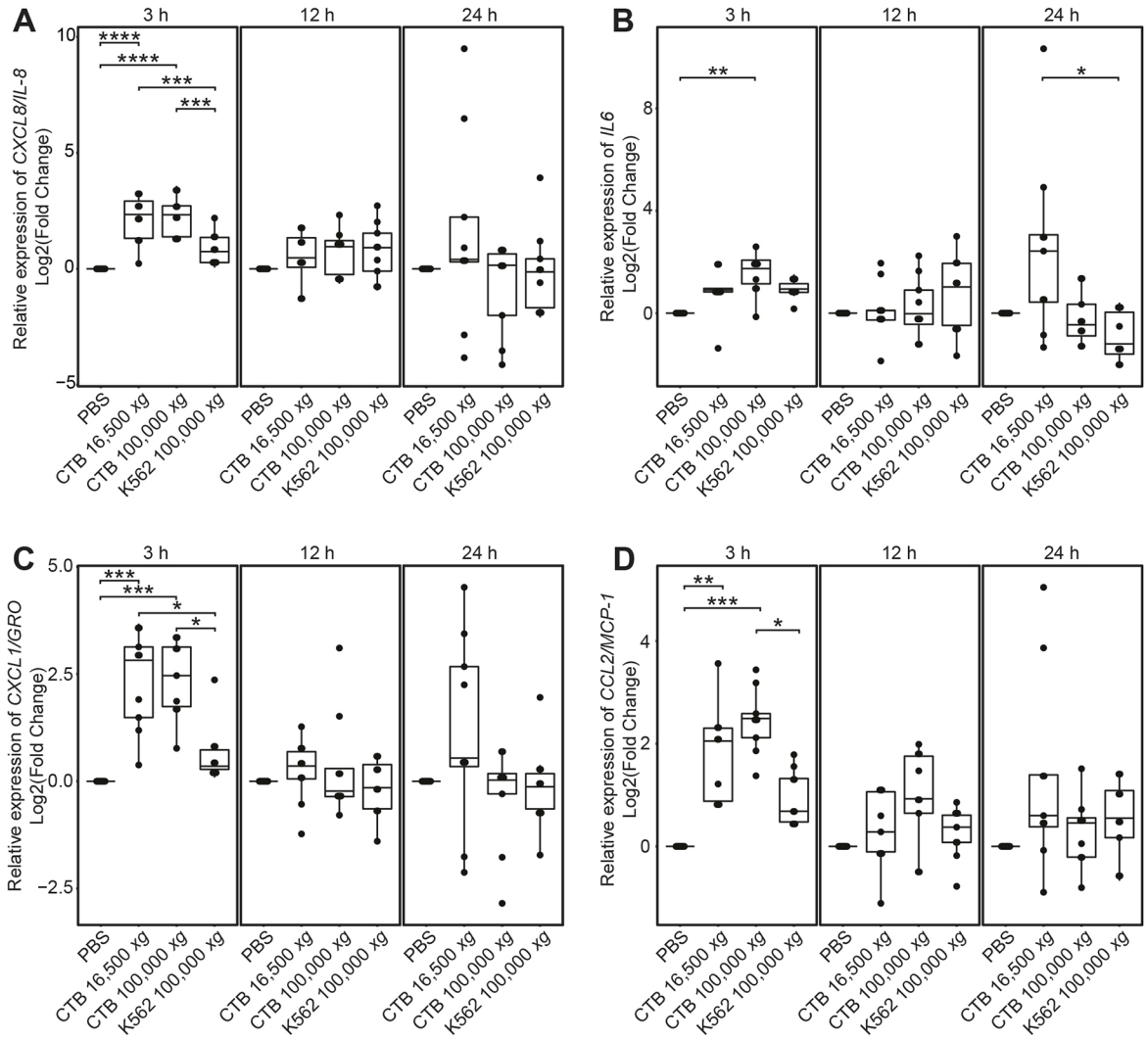

Fig. 6. Quantification of CTB EV effects on dESF expression of mRNAs encoding NF-κB targets. (A-D) Relative mRNA expression of selected NF-κB targets *IL8* (A), *IL6* (B), *CXCL1* (C) and *CCL2* (D). Data for the remaining upregulated analytes (Fig. 5) are displayed in Fig. S2. Compared with the PBS control, CTB 100,000 ***g*** EVs increased dESF transcription of *IL8*, *IL6*, *CXCL1* and *CCL2* at 3 h. Similarly, CTB 16,500 ***g*** EVs increased expression of *IL8*, *CXCL1* and *CCL2* at the same time point. K562 100,000 ***g*** EVs had no effect. *n*=3 biological replicates (EV batches and dESFs). **P*<0.05, ***P*<0.01, ****P*<0.005, *****P*<0.001 (one-way ANOVA with Bonferroni correction).

TNFα associated with CTB 100,000 *g* EVs increased dESF IL8 secretion

Next, we investigated whether TNFα was required for the observed effects of the CTB 100,000 ***g*** EVs on dESF secretion of the NF-κB target IL8. Initially, we used neutralizing anti-TNFα antibodies as inhibitors, but those experiments were unsuccessful. Thus, we asked whether the vesicle contents included receptors for the fragment crystallizable (FC) region of antibodies, which trophoblast cells are known to express (Saji et al., 1999; Simister et al., 1996). Immunoblotting revealed that CTB 100,000 ***g*** EVs included bands of the appropriate molecular weight that reacted with an antibody against the neonatal FC receptor (FcRn; Fig. S6) (Simister and Mostov, 1989).

As an alternative to neutralizing antibodies, we asked whether a soluble form of the TNFα receptor TNFR1 (TNFRSF1A), referred to as sTNFR1, could inhibit the effects of CTB 100,000 ***g*** EVs on dESF IL8 secretion (Fig. 8A). As the vesicles were isolated from primary CTBs and their quantity was limited, we focused on the 12 h time point. CTB 100,000 ***g*** EV treatment increased IL8 secretion by 2.1-fold compared with PBS (P<0.05), whereas pre-incubating the vesicles with sTNFR1 returned IL8 secretion to baseline (P<0.005; Fig. 8B). Thus, the observed effects of CTB 100,000 ***g*** EVs on enhanced dESF secretion of IL8, and likely other NF-κB targets, were attributable to TNFα.

DISCUSSION

Here, we characterized second trimester CTB EVs using TEM, immunoblotting, mass spectrometry and cytokine array. The 100,000 ***g*** fraction was enriched for exosomal markers and both EV populations immunoblotted for the placental proteins HLA-G and PLAP. However, the vesicles that were isolated by high-speed centrifugation were unique in their association with fibronectin. Recently, Jeppesen et al. (2019) described this ECM molecule as a contaminant rather than a component of small EVs isolated from certain cell types (Jeppesen et al., 2019). Whether or not this is true for the CTB 100,000 ***g*** fraction, which also contained integrins that bind this molecule, remains to be determined. In either case, as we had too little starting material to implement additional purification

Development (2020) 147, dev187013. doi:10.1242/dev.187013

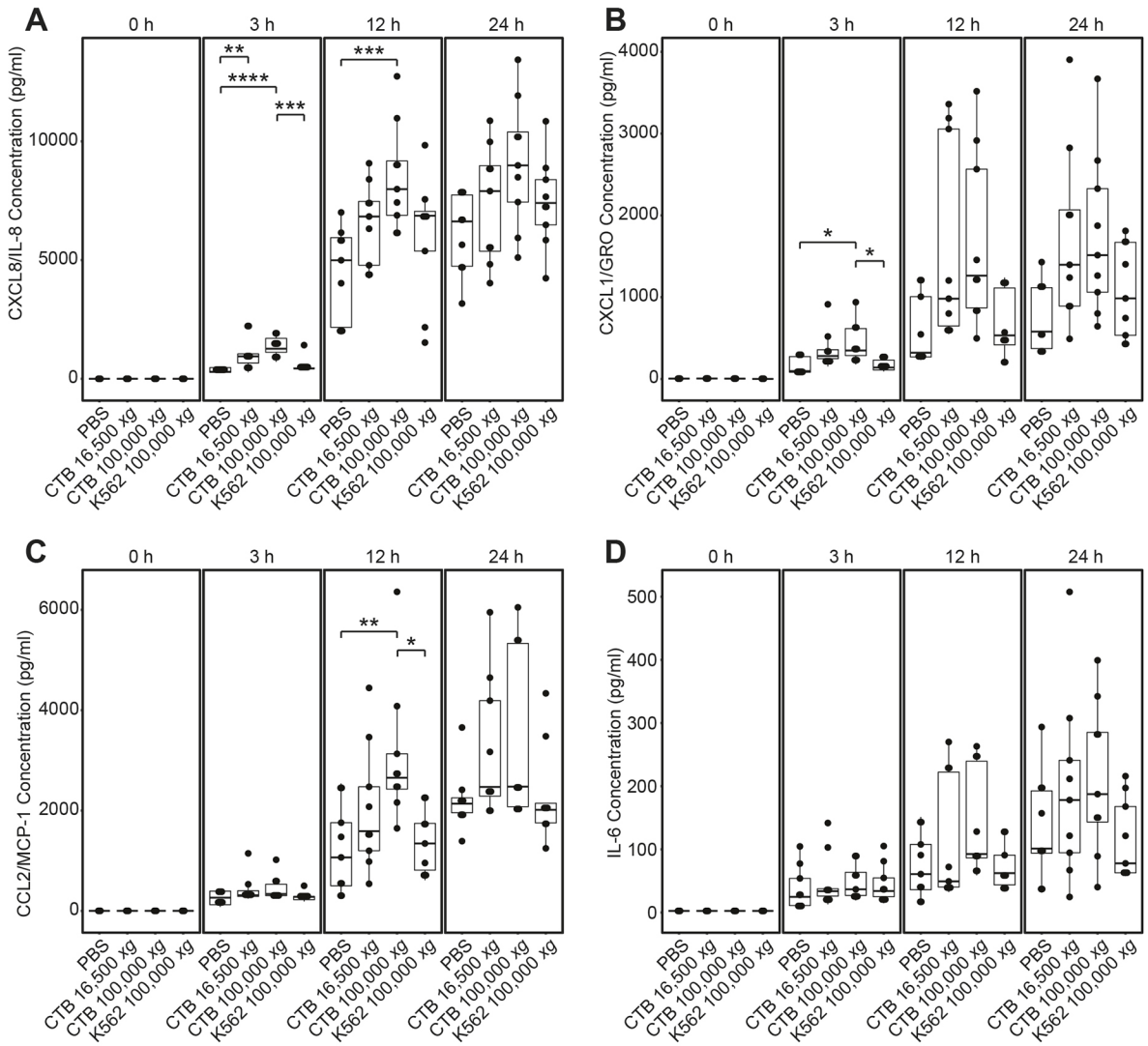

Fig. 7. Treatment with CTB 100,000 *g* EVs enhanced dESF secretion of cytokines. (A-D) Conditioned medium collected at 0, 3, 12 and 24 h from dESFs treated with CTB 16,500 ***g*** EVs, CTB 100,000 ***g*** EVs, K562 100,000 ***g*** EVs and PBS was analyzed by cytokine array. All analytes were significantly increased by CTB EV treatment over the course of the experiment using a generalized linear model (P<0.001). (A) CTB 100,000 ***g*** EVs significantly increased dESF IL8 secretion at 3 and 12 h compared with the PBS or K562 controls. CTB 16,500 ***g*** vesicles significantly increased this cytokine at 3 h. (B) CTB 100,000 ***g*** EVs significantly increased dESF secretion of CXCL1 at 3 h compared with the PBS or K562 controls. (C) CTB 100,000 ***g*** EVs enhanced dESF release of CCL2 at 12 h compared with the controls. (D) IL6 levels in the conditioned medium were not significantly different from the PBS control at any individual time point. n=3 biological replicates (EV batches and dESFs). *P<0.05, **P<0.01, ***P<0.005, ****P<0.001 (one-way ANOVA with Dunnett's test).

steps beyond centrifugation, these EVs likely included other associated rather than intrinsic components.

We also report the discovery of TNFα in CTB 100,000 ***g*** EVs. These vesicles increased decidual cell transcription and secretion of NF-κB target cytokines: IL8, IL6, CCL2 and CXCL1. However, not all targets upregulated by CTB-conditioned medium were significantly increased by EVs (Hess et al., 2007). rhTNFα mimicked the ability of EVs to enhance transcription of NF-κB target genes and secretion of IL8. A soluble form of the TNFα receptor inhibited the ability of CTB 100,000 ***g*** EVs to increase dESF secretion of IL8, linking TNFα with decidual cell release of this chemokine. These results suggest that CTBs have several ways of communicating with uterine cells, which include direct (e.g. cell-cell contact) and indirect (e.g. soluble factors and EVs) means. If the vesicles are transported in a retrograde manner back to the fetus, they could also have effects, most likely on the vasculature that is in direct contact with the blood in which they would be carried.

The interior of 100,000 ***g*** EVs is a non-reducing environment, in which protein disulfide-isomerases catalyze formation of disulfide bonds and multimerization of molecules, which can enhance their activity (Bulleid and Ellgaard, 2011; Lynch et al., 2009). Compared with the cytoplasm, these vesicles contain lower levels of glutathione, which prevents formation of these bonds (Lynch et al., 2009). Other groups have found dimerized molecules in vesicles – a human EBV-transformed B cell line produces 100,000 ***g*** EVs enriched for dimerized classical MHC class I molecules (Lynch et al., 2009). Mouse neuraminidase 1-null myofibroblasts secrete exosomes containing TGF-β1 dimers (van de Vlekkert et al., 2019). In this study, immunoblotting for anti-TNFα demonstrated that the CTB 100,000 ***g*** pellet contains a protein consistent in size with the trimeric form of this molecule (data not shown). We also identified HLA-G dimers in CTB EVs at much higher levels than seen in cell lysates (Fig. 2C). Dimerization of this CTB MHC class I molecule increases its affinity for the

Development (2020) 147, dev187013. doi:10.1242/dev.187013

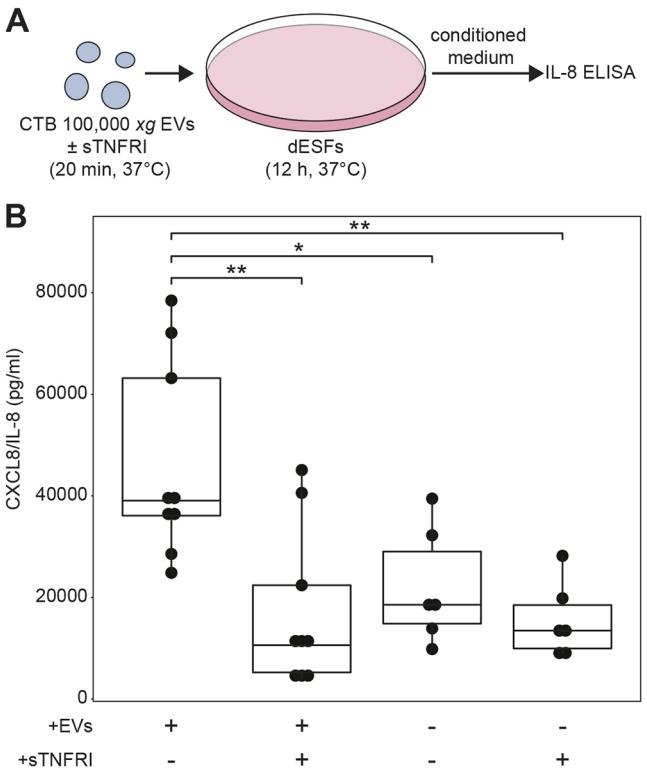

Fig. 8. CTB 100,000 *g* EV stimulation of dESF IL8 secretion was abolished by TNFα inhibition. (A) Schematic of the experimental design. CTB 100,000 ***g*** EVs were pre-incubated with a soluble form of the TNFα receptor (sTNFRI) for 20 m at 37°C before addition to dESFs. After 12 h culture, conditioned medium was collected and analyzed by an ELISA for IL8. (B) sTNFRI pre-treatment of CTB 100,000 ***g*** EVs abolished increased dESF IL8 secretion after 12 h of culture as measured by ELISA (*P<0.05, **P<0.005; one-way ANOVA with Dunnett's test). n=3 biological replicates (EV batches and dESFs).

inhibitory receptors LILRB1 and LILRB2 and, consequently, their signaling strength (Boyson et al., 2002; Kovats et al., 1990; Shiroishi et al., 2006; Yelavarthi et al., 1991). We detected multiple protein disulfide-isomerases in both CTB EV types using mass spectrometry, suggesting that they promote dimerization of vesicular proteins. Furthermore, CTB HLA-G is heavily glycosylated with polylactosamine chains, which are composed of N-acetylglucosamine-galactose dimers (McMaster et al., 1998). These residues are recognized by CD206 (MRC1), an inhibitory mannose receptor present on decidual macrophages (Co et al., 2013). Thus, CTB EV expression of dimeric HLA-G may be a key component of the mechanisms that mediate maternal tolerance to the fetus.

TNFα, IL8, CCL2, CXCL1 and their receptors are present at the maternal-fetal interface at early and mid-gestation in humans, bolstering the *in vivo* relevance of this study. Anti-TNFα immunolocalizes to first and second trimester invasive and endovascular CTBs and decreases to only weak staining in spiral arteries at term (Pijnenborg et al., 1998). *In situ* hybridization revealed that the decidual stroma uniformly expresses *CXCL1*, whereas *CCL2* localizes strongly to isolated patches of these cells, with other areas exhibiting a diffuse signal (Red-Horse et al., 2001). In terms of receptors, CTBs immunostain with anti-CXCR1 (IL8 receptor) by immunohistochemistry and variably express mRNAs for *CXCR2* (*IL8* and *CXCL1* receptor) and *CCR2* (*CCL2* receptor), indicating that dESF cytokines may be part of a network of paracrine signals that can influence CTBs (Drake et al., 2004; Hanna et al., 2006). Decidual leukocytes express mRNAs for *CCR4* (*CCL2* receptor) consistently and for *CXCR1* and *CXCR2* variably (Red-Horse et al., 2001), suggesting a role for recruitment of immune cells to the maternal-fetal interface.

CTB EV-induced dESF cytokine secretion may play important roles in CTB migration. IL8 increases first trimester primary CTB migration, whereas CCL2 has no effect (Hanna et al., 2006). Another study found that IL6 secreted by endometrial cells is partially responsible for promoting migration of trophoblast cell lines *in vitro* (Dominguez et al., 2008). CTB EV-induced dESF cytokine secretion may also play a role in immune cell recruitment to the decidua. For example, CCL2 is a chemoattractant for monocytes, NK cells and T cells (Allavena et al., 1994; Carr et al., 1994; Matsushima et al., 1989; Valente et al., 1988). Thus, the CTB EV-dESF interactions have effects on other cell types that play important roles in pregnancy outcomes.

Based on studies of the biological activities of CTB-conditioned medium, EVs likely have broader functional effects on the uterine environment. CTBs secrete factors that promote lymphangiogenesis via a mechanism that partially depends on TNFα (Red-Horse et al., 2006). First trimester CTB-conditioned medium induces peripheral monocyte differentiation into macrophages and alters their ability to secrete cytokines (Aldo et al., 2014). CTB-secreted factors induce apoptosis of smooth muscle cells in spiral arteries via Fas ligand, a transmembrane protein that has been identified in CTB EVs (Abrahams et al., 2004; Harris et al., 2006). Thus, although we focused on the function of TNFα in the context of CTB EVs, we believe that this molecule is one of many that can play important roles in modulation of the uterine environment, with possible systemic effects.

Although an inflammatory response at implantation is conserved across mammalian species (Griffith et al., 2017), inhibition of most cytokines does not prevent implantation in mice and humans, suggesting redundant pathways. Individual genetic deletions of *TNF*, *IL6*, *CXCL1* or *CCL2* result in fertile mice with normal litter sizes (Boisvert et al., 2006; Lu et al., 1998; Marino et al., 1997; Pasparakis et al., 1996; Robertson et al., 2010). However, suppression of uterine NF-κB activity with an inhibitory subunit of the complex delays implantation by 1 day in mice (Nakamura et al., 2004). TNFα and IL6 inhibitors are prescribed to treat human autoimmune diseases, and women on these biologic therapies have live births. However, even transient treatment with TNFα inhibitors during pregnancy may increase the risk of birth defects and preterm labor, but it is difficult to separate TNFα effects and those of underlying maternal diseases (Johansen et al., 2018). Data on IL6 inhibition during pregnancy are more limited and drawn from smaller sample sizes. Results to date suggest an increased risk of preterm birth but not fetal anomalies (Hoeltzenbein et al., 2016). Overall, these findings suggest redundant mechanisms; simultaneous blockade of multiple cytokines may be required to negatively impact implantation and maintenance of pregnancy.

In addition to implantation, parturition is associated with an inflammatory response across species. Genetic deletion of *IL6* in mice results in a 24 h delay in birth, which is restored to normal with administration of recombinant IL6 (Robertson et al., 2010). In humans, IL8 is upregulated at parturition in the myometrium and the decidua, where it localizes to the stroma and may have a role in cervical dilation (Osmers et al., 1995; Sakamoto et al., 2004). Microarray analyses showed that labor increases term decidual expression of *TNFAIP3*, *IL6*, *NFKBIA* and other NF-κB targets (Rinaldi et al., 2017). In addition, labor increases decidual expression of IL8, while decreasing that of CCL2 (El-Azzamy

Development (2020) 147, dev187013. doi:10.1242/dev.187013

et al., 2017). Thus, the ability of CTB EVs to modulate the expression of NF-κB targets across gestation could have important effects at many stages of pregnancy.

Compared with STB EVs, those released by CTBs are likely to have different effects. One factor is sheer numbers. STBs form the entire surface of the placenta, estimated to be ∼12 m^2 at term (Boyd, 1984), making them an abundant source of EVs. In contrast, CTBs, which fuse to form STBs or differentiate into the extravillous subpopulation, are depleted as pregnancy advances. Thus, we believe CTBs likely release, in total, fewer EVs than STBs, especially towards term. In addition, they have substantially different proteomes. Comparison of the mass spectrometry data for CTB 100,000 ***g*** EVs (Table S2) and an equivalent STB fraction (Baig et al., 2014) showed an overlap of ∼30%, supporting the theory that there are also substantial functional differences.

Preeclampsia increases circulating levels of placental EVs (Germain et al., 2007; Knight et al., 1998; Lok et al., 2008). Perfusion-derived STB EVs from preeclamptic and normal placentas differ in contents and function. For example, in preeclampsia, STB EVs contain increased levels of Flt1 and the percentage of endoglin-containing vesicles decreases (Tannetta et al., 2013). These molecules with angiogenic effects may contribute to the perturbation of maternal vasculature responses that are the hallmark of this pregnancy complication (Tannetta et al., 2013). These EVs also contain reduced levels of endothelial nitric oxide synthase and nitric oxide (Motta-Mejia et al., 2017). In addition, preeclampsia STB EVs have an increased ability to activate platelets (Tannetta et al., 2015). Overall, it is unclear whether vesicles contribute to the pathology of the disease or are a compensatory mechanism for a failing placenta.

As CTBs are in direct contact with maternal blood, they likely secrete EVs into circulation to mediate pregnancy associated changes throughout the mother's body. For example, many organs enlarge during pregnancy. Blood volume expands by almost 50% (Hytten, 1985). The liver increases in size to meet the enhanced demands of the embryo/fetus (Hollister et al., 1987). In mice, pregnancy stimulates neurogenesis in the maternal olfactory bulb via a prolactin-mediated mechanism (Medina and Workman, 2018; Shingo et al., 2003). Pregnant women develop insulin resistance, increasing glucose availability for the growing embryo/fetus and requiring the maternal pancreas to secrete higher levels of insulin (Lain and Catalano, 2007). The mechanism underlying pancreatic adaptation to pregnancy is unknown. Thus, placental EVs may play a role in a subset of these maternal responses to pregnancy. Additional studies will focus on a role for CTB EVs in mediating distant physiologic changes required for reproductive success.

MATERIALS AND METHODS

Tissue collection

The University of California, San Francisco (UCSF) Institutional Review Board approved this study. All donors gave informed consent. Second trimester placentas were collected immediately following elective terminations and placed in cytowash medium, containing DME/H-21, 12.5% fetal bovine serum (FBS; Hyclone), 1% glutamine plus (Atlanta Biologicals), 1% penicillin/streptomycin and 0.1% gentamicin. Tissue samples were placed on ice before dissection.

Isolation and culture of human primary CTBs

CTBs were isolated from second trimester human placentas as previously described (Hunkapiller and Fisher, 2008). Single cells were counted using a hemocytometer and immediately plated on Matrigel (BD Biosciences)-coated 6-well plates in 1.5ml serum-free medium containing DME/H-21, 2% Nutridoma-SP (Roche), 1% sodium pyruvate, 1% HEPES buffer, 1% glutamine plus, 1% penicillin/streptomycin and 0.1% gentamicin. CTBs were cultured at a density of between 8×10^5 and 1.5×10^6 cells/well. CTBs were incubated at 37°C in 5% CO_2/95% air. After 1 h, the medium with unattached immune and other cells was removed and replaced with another 3 ml serum-free medium before returning the cells to the incubator.

K562 cell culture

Erythroleukemic K562 cells were previously grown in the Fisher lab (Co et al., 2013) and tested negative for mycoplasma. K562 cultures were seeded with 1×10^5 cells per ml Iscove's Modified Dulbecco's Medium containing 10% FBS. They were grown in 15 cm dishes at 37°C in 5% CO_2/95% air. For EV isolation, K562 cells were pelleted at 400 ***g*** and resuspended (1×10^5 cells/ml) in AIM-V serum-free medium (Gibco).

Isolation of EVs

EVs were isolated by differential centrifugation at 4°C using previously published methods (Théry et al., 2006). After culturing for 36-38 h, conditioned medium was centrifuged at 400 ***g*** for 5 min to pellet the cells. The supernatant was sequentially centrifuged at 2000 ***g*** and 16,500 ***g***, each for 20 min. The liquid fraction was passed through a 0.22 µm filter before ultracentrifugation at 100,000 ***g*** for 70 min. The supernatant was removed by aspiration. The 16,500 ***g*** and 100,000 ***g*** pellets were resuspended in 35 ml PBS and re-centrifuged under the original conditions with which they were collected. The pellet was isolated by aspiration of the liquid phase. Typically, 5 µl was reserved to determine the protein concentration and the remaining 70 µl was used in experiments. Both aliquots were stored at −80°C. Samples for protein determinations were lysed in an equivalent volume of buffer containing 100 mM ammonium bicarbonate and 0.2% SDS. Quantitation was accomplished using a Micro BCA Protein Assay kit (Thermo Scientific Pierce).

TEM

TEM was performed as previously described (Théry et al., 2006). In brief, EVs were adsorbed onto a glow discharged 400 mesh Formvar-coated copper grid (Electron Microscopy Sciences) for 1 min. Samples were negatively stained by dipping four times in 1% aqueous uranyl acetate. Excess liquid was blotted with filter paper. Grids were air dried and imaged in a Tecnai 12 transmission electron microscope (Field Electron and Ion Company).

Immunoblotting and immunofluorescence

EVs or cell lysates were lysed as described above. For all targets except FcRn, 2 µg protein was dissolved under non-reducing conditions with NuPAGE LDS Sample Buffer (Invitrogen). For FcRn, 10 µg protein was solubilized in NuPAGE LDS Sample Buffer containing 0.1 M dithiothreitol (DTT). Samples were boiled for 10 min, separated on a NuPAGE 4-12% Bis-Tris gel (Invitrogen) and transferred to a 0.45 µm nitrocellulose membrane (Bio-Rad). Blocking was accomplished with 5% powdered nonfat dry milk reconstituted in PBS-T (0.1% Tween in PBS). Membranes were incubated in primary antibody diluted in blocking buffer at 4°C overnight. The isotype, dilution and source for each of the primary and secondary antibodies is summarized in Table S3. Immunoreactive bands were visualized with ECL2 Western blotting substrate (Thermo Scientific Pierce), and Amersham Hyperfilm ECL (GE Healthcare).

Immunofluorescence was performed as previously described (Robinson et al., 2017). Briefly, tissue was fixed in 4% paraformaldehyde and dehydrated by passing through sequential solutions containing increasing sucrose concentrations before embedding in OCT (Thermo Fisher Scientific). Sections (15 µm) were incubated with rat anti-cytokeratin 7 (Damsky et al., 1992) to label CTBs and another primary antibody diluted at 1:100 (vol/vol) in blocking buffer (PBS with 3% bovine serum albumin) for 1 h at room temperature. Primary antibodies were detected with species-specific secondary antibodies. Primary and secondary antibodies and their sources are described in Table S3. Sections were washed in PBS and mounted with Vectashield containing 4′6-diamidino-2-phenylindole (DAPI; Vector Biolabs). Samples were visualized with a Leica SP5 confocal microscope or a Leica DM5000 B inverted microscope. Tissue sections from three placentas were evaluated.

Development (2020) 147, dev187013. doi:10.1242/dev.187013

Mass spectrometry analyses

EV samples were lysed as described above. Lysates were prepared that contained a minimum of 25 µg protein, sometimes achieved by pooling. Samples were reduced with tris(2-carboxyethyl) phosphine hydrochloride (TCEP) added to a final concentration of 5 mM at 60°C for 1 h and immediately alkylated with freshly prepared iodoacetamide (IAA) at a final concentration of 10 mM for 15 min at room temperature. Digestion was performed by incubating samples overnight with 3 µg sequencing-grade trypsin (Promega) at 37°C. SDS was removed with 2 ml Detergent Removal Columns (Pierce). Samples were stored frozen at −80°C before analysis.

Samples were analyzed by reverse-phase HPLC-ESI-MS/MS using the Eksigent Ultra Plus nano-LC 2D HPLC system combined with a cHiPLC system directly connected to an orthogonal quadrupole time-of-flight SCIEX TripleTOF 6600 mass spectrometer (SCIEX). Typically, mass resolution in precursor scans was ∼45,000 (TripleTOF 6600), whereas fragment ion resolution was ∼15,000 in 'high sensitivity' product ion scan mode. After injection, peptide mixtures were transferred onto a C18 pre-column chip (200 µm×6 mm ChromXP C18-CL chip, 3 µm, 300 Å, SCIEX) and washed at 2 µl/min for 10 min with the loading solvent (H_2O/0.1% formic acid) for desalting. Peptides were transferred to the 75 µm×15 cm ChromXP C18-CL chip, 3 µm, 300 Å, (SCIEX), and eluted at 300 nl/min with a 3 h gradient using aqueous and acetonitrile solvent buffers (Schilling et al., 2015).

All samples were analyzed by data-independent acquisitions (DIA), specifically using variable window DIA acquisitions (Collins et al., 2017). For these acquisitions, windows of variable width (5 to 90 m/z) were passed in incremental steps over the full mass range (m/z 400-1250). The cycle time of 3.2 s included a 250 ms precursor ion scan followed by a 45 ms accumulation time for each of the 64 DIA segments. The variable windows were determined according to the complexity of the typical MS1 ion current observed within a certain m/z range using a SCIEX 'variable window calculator' algorithm. Narrower windows were chosen in 'busy' m/z ranges; wider windows were chosen in m/z ranges with few eluting precursor ions (Schilling et al., 2017). DIA tandem mass spectra produced complex MS/MS spectra, which were a composite of all the analytes within each selected Q1 m/z window.

Processing, quantification and statistical analysis of MS data

DIA acquisitions were quantitatively processed using the proprietary Spectronaut v12 (12.020491.3.1543) software from Biognosys (Bruderer et al., 2015). A pan-human spectral library that provided quantitative DIA assays for ∼10,000 human proteins was used for Spectronaut processing (Rosenberger et al., 2014). Quantitative DIA MS2 data analysis was based on extracted ion chromatograms (XICs) of 6-10 of the most abundant fragment ions in the identified spectra. Relative quantification was performed comparing different samples to assess fold changes.

GO analyses

Redundancies were collapsed according to the total number of peptides. We performed functional enrichment of GO Biological Processes (Level 4) of the EV proteomes as defined by gene symbols using DAVID (Huang et al., 2007).

Profiling EV cytokines

To identify cytokine contents, 2 µg of EV protein was diluted to 1 ml with ESF medium containing 2% charcoal-stripped FBS, DMEM, insulin 0.5%, and MCDB 105 medium. The samples were profiled with the $MILLIPLEX_{MAP}$ Human High Sensitivity T Cell Panel (Millipore, HSTCMAG-28SK) on a Luminex LX 200 analyzer using Bio-Plex manager software 6.1.1 (Bio-Rad).

Endometrial stromal fibroblast culture and decidualization

Human endometrial samples were collected from the UCSF/National Institutes of Health Human Endometrial Tissue and DNA Bank after written informed consent. Endometrial stromal fibroblasts (ESFs) were isolated from endometrial biopsies (n=20). They were washed in PBS and digested with collagenase IV for 1 h at 37°C with constant shaking. The digests were size fractionated by passing through a 40 µm filter. The primary cells present in the filtrate and subsequent passages were cultured in stromal cell medium: 10% charcoal-stripped FBS-containing medium, DMEM, 1 mM sodium pyruvate, 5 µg/ml final concentration insulin and MCDB 105 medium (Irwin et al., 1989). Only morphologically homogenous ESF cell cultures as determined by microscopic examination were used in experiments. Before decidualization, cultured ESFs were serum-starved for 24 h in 2% charcoal-stripped FBS-containing medium without insulin. Then they were treated with 10 nM E2 and 1 µM P4 (E2P4 medium) or the vehicle control for 14-21 days (Houshdaran et al., 2014). Decidualization was assessed using an ELISA to quantify IGFBP1 secretion into the medium (Alpha Diagnostic International, 0900) and by microscopic examination to assess morphologic changes. The three ESF cell lines exhibiting the most robust decidualization were used in the initial screens. The subsequent functional assays also employed the same three ESF lines, which were frozen, thawed and decidualized for each set of experiments.

EV effects on the ESF secretome and the role of TNFα

In these experiments, the effects of EVs from three CTB cultures established from different placentas were analyzed. A portion of each EV fraction that was aliquoted in PBS was added to the hormone-containing ESF medium to a final concentration of 2 µg per ml. Typically, 10 ml batches were prepared. A portion (500 µl) was reserved as a control for downstream analyses and 1 ml was added to each dESF well. The cells were cultured for 3, 12 or 24 h, at which point conditioned medium was collected and centrifuged at 400 ***g***. The supernatant was stored at −80°C. The cells were washed with PBS, detached from the plate by treatment with 0.25% trypsin with EDTA in PBS (Ca^{++}/Mg^{++}-free) and pelleted by centrifugation at 400 ***g***. The pellets were flash frozen in a dry ice-ethanol slush and stored (−80°C).

Samples of dESF RNA were prepared for analysis using a chip-based method of qRT-PCR using a 96.96 Dynamic Array integrated fluidic circuit (IFC; Fluidigm) according to the manufacturer's protocol. Total RNA was isolated from frozen cell pellets with a NucleoSpin RNA isolation kit (Machery-Nagel). The concentration and quality were estimated using a Nanodrop spectrophotometer (Thermo Fisher Scientific). cDNA libraries were prepared with 150 ng RNA using Reverse Transcription Master Mix (Fluidigm) and pre-amplified with Preamp Master Mix (Fluidigm) and pooled delta gene assay mix (500 nm; Fluidigm). The samples were digested with exonuclease I (New England BioLabs), and diluted 1:10 (vol/vol) in 1× DNA suspension buffer (TEKnova). Delta gene assay primer sequences are listed in Table S4. Samples were prepared with 2× SsoFast EvaGreen Supermix with low ROX (Bio-Rad) and 20× DNA Binding Dye (Fluidigm). Primer mixes contained 2× Assay Loading Reagent (Fluidigm), 1× DNA Suspension Buffer, and Delta gene assay combined forward and reverse primers (100 µM). After priming and loading the 96.96 chip using an IFC Controller HX (Fluidigm), qRT-PCR data were collected on a Biomark instrument (Fluidigm). Statistics were performed on dCt values, calculated as the difference in Ct values between the gene of interest and the average of two housekeeping genes: *HSP90AB1* and *G6PD*. Differential expression between EV treatments and controls was calculated via the ΔΔCT method: normalized to the mean of housekeeping genes and adjusted to the PBS control for each ESF line, EV batch and time point.

We measured changes in dESF NF-κB target secretion in response to EV treatment using a custom $MILLIPLEX_{MAP}$ Human Cytokine/Chemokine Magnetic Bead Panel (Millipore, HCYTOMAG-60K) to assay conditioned medium for IL8, IL6, CCL2 and CXCL1. These experiments employed a Luminex LX 200 analyzer and the data were generated using Bio-Plex manager software 6.1.1 (Bio-Rad).

To determine the effects of rhTNFα, the lyophilized protein (R&D Systems, 210-TA-005) was reconstituted in PBS to a concentration of 0.1 mg/ml. This working solution was serially diluted to a final concentration of 1 pg/ml, 10 pg/ml or 100 pg/ml in E2P4 medium. rhTNFα-containing medium (1 ml) was added to each well of dESFs. As a control, some wells contained E2P4 medium alone. Conditioned medium and cell pellets for RNA isolation were collected after 3, 12 or 24 h of culture as described above.

IL8 levels were measured using a Quantikine ELISA Kit (R&D Systems, S8000C) according to the manufacturer's instructions. Samples were diluted

1:20 in calibrator diluent RD5P. According to the manufacturer's instructions, a face mask was worn during the assay to prevent IL8 contamination from saliva.

For TNFα inhibition experiments, sTNFR1 (R&D Systems, 636-R1-025) was reconstituted in PBS. EVs diluted in E2P4 medium as described above were incubated with or without sTNFR1 (1 µg/ml) for 20 min at 37°C. An aliquot (1 ml) was added to each dESF well. After 12 h, conditioned medium was collected as described above.

Statistics

Statistical analyses were performed using SPSS version 24 (IBM). The high-sensitivity T cell cytokine array and mRNA data were analyzed using a one-way ANOVA with Bonferroni correction. The immunoblot densitometry measurements, the ESF cytokine array data at individual time points and the IL8 ELISAs were analyzed using a one-way ANOVA with Dunnett's test. We also used a generalized linear model of cytokine secretion for the time course experiment with time, cell line, EV batch and treatment as independent variables.

Acknowledgements

We thank Yan Zhou, Sirirak Buarpung, Hao Chen, Kim Chi Vo, Sushmita Sen, Juan Irwin and Yvonne Kim for their technical assistance and insight; the recruiters; the patient participants; Harry Slomovits and Norma McCormack for administrative support; Michael McMaster for careful reading of this manuscript; and Lewis Lanier, Robert Blelloch, and Adrian Erlebacher for their insight and suggestions. We also thank the following core facilities: Danielle Jorgens and Reena Zalpuri at the University of California Berkeley Electron Microscope Laboratory for training and assistance in TEM sample preparation and data collection; John Heitman at the Vitalant Research Institute Core Immunology Laboratory for performing cytokine arrays; and Iryna Lobach at the UCSF Clinical & Translational Science Institute for insight and direction in statistical analyses. A portion of the data and text in this paper were part of a Ph.D. thesis (S.K.T.) that was completed in 2019 at the University of California San Francisco.

Competing interests

S.J.F. is a consultant for Novo Nordisk.

Author contributions

Conceptualization: S.K.T., S.H., M.J.G., L.C.G., S.J.F.; Methodology: S.K.T., S.H., E.Y.K., M.K., B.S., S.J.F.; Software: S.K.T.; Validation: S.K.T., M.J.G.; Formal analysis: S.K.T., J.F.R., M.J.G., B.S.; Investigation: S.K.T., S.H., M.J.G., E.Y.K., M.K., B.S.; Resources: L.C.G., S.J.F.; Writing - original draft: S.K.T., S.H., B.S., S.J.F.; Writing - review & editing: S.K.T., S.H., J.F.R., L.C.G., S.J.F.; Visualization: S.K.T., M.J.G., E.Y.K.; Supervision: L.C.G., S.J.F.; Project administration: S.K.T., L.C.G., S.J.F.; Funding acquisition: L.C.G., S.J.F.

Funding

This work was kindly supported by the National Institutes of Health (T32HD007470 to S.K.T.; P50 HD055764 to L.C.G. and S.J.F.). This publication was also supported by the National Center for Advancing Translational Sciences, National Institutes of Health, through UCSF-CTSI Grant Number UL1 TR001872. Deposited in PMC for release after 12 months.

Data availability

All raw files have been uploaded to the Center for Computational Mass Spectrometry, MassIVE (https://massive.ucsd.edu) under the accession number: MSV000085274. Data uploads include the protein identification details.

Supplementary information

Supplementary information available online at
https://dev.biologists.org/lookup/doi/10.1242/dev.187013.supplemental

Peer review history

The peer review history is available online at
https://dev.biologists.org/lookup/doi/10.1242/dev.187013.reviewer-comments.pdf

References

Abed, M., Verschueren, E., Budayeva, H., Liu, P., Kirkpatrick, D. S., Reja, R., Kummerfeld, S. K., Webster, J. D., Gierke, S., Reichelt, M. et al. (2019). The Gag protein PEG10 binds to RNA and regulates trophoblast stem cell lineage specification. *PLoS ONE* **14**, e0214110. doi:10.1371/journal.pone.0214110

Abrahams, V. M., Straszewski-Chavez, S. L., Guller, S. and Mor, G. (2004). First trimester trophoblast cells secrete Fas ligand which induces immune cell apoptosis. *Mol. Hum. Reprod.* **10**, 55-63. doi:10.1093/molehr/gah006

Alam, S. M. K., Jasti, S., Kshirsagar, S. K., Tannetta, D. S., Dragovic, R. A., Redman, C. W., Sargent, I. L., Hodes, H. C., Nauser, T. L., Fortes, T. et al. (2018). Trophoblast Glycoprotein (TPGB/5T4) in human placenta: expression, regulation, and presence in extracellular microvesicles and exosomes. *Reprod. Sci.* **25**, 185-197. doi:10.1177/1933719117707053

Aldo, P. B., Racicot, K., Craviero, V., Guller, S., Romero, R. and Mor, G. (2014). Trophoblast induces monocyte differentiation into CD14+/CD16+ macrophages. *Am. J. Reprod. Immunol.* **72**, 270-284. doi:10.1111/aji.12288

Allavena, P., Bianchi, G., Zhou, D., van Damme, J., Jilek, P., Sozzani, S. and Mantovani, A. (1994). Induction of natural killer cell migration by monocyte chemotactic protein-1, −2 and −3. *Eur. J. Immunol.* **24**, 3233-3236. doi:10.1002/eji.1830241249

Anisowicz, A., Messineo, M., Lee, S. W. and Sager, R. (1991). An NF-kappa B-like transcription factor mediates IL-1/TNF-alpha induction of gro in human fibroblasts. *J. Immunol.* **147**, 520-527.

Baig, S., Kothandaraman, N., Manikandan, J., Rong, L., Ee, K. H., Hill, J., Lai, C. W., Tan, W. Y., Yeoh, F., Kale, A. et al. (2014). Proteomic analysis of human placental syncytiotrophoblast microvesicles in preeclampsia. *Clin. Proteomics* **11**, 40. doi:10.1186/1559-0275-11-40

Boisvert, W. A., Rose, D. M., Johnson, K. A., Fuentes, M. E., Lira, S. A., Curtiss, L. K. and Terkeltaub, R. A. (2006). Up-regulated expression of the CXCR2 ligand KC/GRO-α in atherosclerotic lesions plays a central role in macrophage accumulation and lesion progression. *Am. J. Pathol.* **168**, 1385-1395. doi:10.2353/ajpath.2006.040748

Boyd, P. A. (1984). Quantitative structure of the normal human placenta from 10 weeks of gestation to term. *Early Hum. Dev.* **9**, 297-307. doi:10.1016/0378-3782(84)90074-4

Boyson, J. E., Erskine, R., Whitman, M. C., Chiu, M., Lau, J. M., Koopman, L. A., Valter, M. M., Angelisova, P., Horejsi, V. and Strominger, J. L. (2002). Disulfide bond-mediated dimerization of HLA-G on the cell surface. *Proc. Natl. Acad. Sci. USA* **99**, 16180-16185. doi:10.1073/pnas.212643199

Brach, M. A., Henschler, R., Mertelsmann, R. H. and Herrmann, F. (1991). Regulation of M-CSF expression by M-CSF: role of protein kinase C and transcription factor NF kappa B. *Pathobiology* **59**, 284-288. doi:10.1159/000163664

Bren, G. D., Solan, N. J., Miyoshi, H., Pennington, K. N., Pobst, L. J. and Paya, C. V. (2001). Transcription of the RelB gene is regulated by NF-kappaB. *Oncogene* **20**, 7722-7733. doi:10.1038/sj.onc.1204868

Bruderer, R., Bernhardt, O. M., Gandhi, T., Miladinović, S. M., Cheng, L.-Y., Messner, S., Ehrenberger, T., Zanotelli, V., Butscheid, Y., Escher, C. et al. (2015). Extending the limits of quantitative proteome profiling with data-independent acquisition and application to acetaminophen-treated three-dimensional liver microtissues. *Mol. Cell. Proteomics* **14**, 1400-1410. doi:10.1074/mcp.M114.044305

Bulleid, N. J. and Ellgaard, L. (2011). Multiple ways to make disulfides. *Trends Biochem. Sci.* **36**, 485-492. doi:10.1016/j.tibs.2011.05.004

Carr, M. W., Roth, S. J., Luther, E., Rose, S. S. and Springer, T. A. (1994). Monocyte chemoattractant protein 1 acts as a T-lymphocyte chemoattractant. *Proc. Natl. Acad. Sci. USA* **91**, 3652-3656. doi:10.1073/pnas.91.9.3652

Co, E. C., Gormley, M., Kapidzic, M., Rosen, D. B., Scott, M. A., Stolp, H. A. R., McMaster, M., Lanier, L. L., Barcena, A. and Fisher, S. J. (2013). Maternal decidual macrophages inhibit NK cell killing of invasive cytotrophoblasts during human pregnancy. *Biol. Reprod.* **88**, 155. doi:10.1095/biolreprod.112.099465

Collins, B. C., Hunter, C. L., Liu, Y., Schilling, B., Rosenberger, G., Bader, S. L., Chan, D. W., Gibson, B. W., Gingras, A.-C., Held, J. M. et al. (2017). Multi-laboratory assessment of reproducibility, qualitative and quantitative performance of SWATH-mass spectrometry. *Nat. Commun.* **8**, 291. doi:10.1038/s41467-017-00249-5

Costa-Silva, B., Aiello, N. M., Ocean, A. J., Singh, S., Zhang, H., Thakur, B. K., Becker, A., Hoshino, A., Mark, M. T., Molina, H. et al. (2015). Pancreatic cancer exosomes initiate pre-metastatic niche formation in the liver. *Nat. Cell Biol.* **17**, 816-826. doi:10.1038/ncb3169

Damsky, C. H. and Fisher, S. J. (1998). Trophoblast pseudo-vasculogenesis: faking it with endothelial adhesion receptors. *Curr. Opin. Cell Biol.* **10**, 660-666. doi:10.1016/S0955-0674(98)80043-4

Damsky, C. H., Fitzgerald, M. L. and Fisher, S. J. (1992). Distribution patterns of extracellular matrix components and adhesion receptors are intricately modulated during first trimester cytotrophoblast differentiation along the invasive pathway, in vivo. *J. Clin. Invest.* **89**, 210-222. doi:10.1172/JCI115565

Delorme-Axford, E., Donker, R. B., Mouillet, J.-F., Chu, T., Bayer, A., Ouyang, Y., Wang, T., Stolz, D. B., Sarkar, S. N., Morelli, A. E. et al. (2013). Human placental trophoblasts confer viral resistance to recipient cells. *Proc. Natl. Acad. Sci. USA* **110**, 12048-12053. doi:10.1073/pnas.1304718110

Dominguez, F., Martinez, S., Quinonero, A., Loro, F., Horcajadas, J. A., Pellicer, A. and Simon, C. (2008). CXCL10 and IL-6 induce chemotaxis in human trophoblast cell lines. *Mol. Hum. Reprod.* **14**, 423-430. doi:10.1093/molehr/gan032

Donker, R. B., Mouillet, J. F., Chu, T., Hubel, C. A., Stolz, D. B., Morelli, A. E. and Sadovsky, Y. (2012). The expression profile of C19MC microRNAs in primary human trophoblast cells and exosomes. *Mol. Hum. Reprod.* **18**, 417-424. doi:10.1093/molehr/gas013

Drake, P. M., Red-Horse, K. and Fisher, S. J. (2004). Reciprocal chemokine receptor and ligand expression in the human placenta: implications for cytotrophoblast differentiation. *Dev. Dyn.* **229**, 877-885. doi:10.1002/dvdy.10477

El-Azzamy, H., Balogh, A., Romero, R., Xu, Y., LaJeunesse, C., Plazyo, O., Xu, Z., Price, T. G., Dong, Z., Tarca, A. L. et al. (2017). Characteristic Changes in Decidual Gene Expression Signature in Spontaneous Term Parturition. *J Pathol Transl Med* **51**, 264-283. doi:10.4132/jptm.2016.12.20

Ellis, S. A., Sargent, I. L., Redman, C. W. and McMichael, A. J. (1986). Evidence for a novel HLA antigen found on human extravillous trophoblast and a choriocarcinoma cell line. *Immunology* **59**, 595-601.

Garrick, M. D. (2011). Human iron transporters. *Genes Nutr.* **6**, 45-54. doi:10.1007/s12263-010-0184-8

Gaw, S. L., Hromatka, B. S., Ngeleza, S., Buarpung, S., Ozarslan, N., Tshefu, A. and Fisher, S. J. (2019). Differential activation of fetal Hofbauer cells in primigravidas is associated with decreased birth weight in symptomatic placental malaria. *Malar Res. Treat.* **2019**, 1378174. doi:10.1155/2019/1378174

Germain, S. J., Sacks, G. P., Soorana, S. R., Sargent, I. L. and Redman, C. W. (2007). Systemic inflammatory priming in normal pregnancy and preeclampsia: the role of circulating syncytiotrophoblast microparticles. *J. Immunol.* **178**, 5949-5956. doi:10.4049/jimmunol.178.9.5949

Griffith, O. W., Chavan, A. R., Protopapas, S., Maziarz, J., Romero, R. and Wagner, G. P. (2017). Embryo implantation evolved from an ancestral inflammatory attachment reaction. *Proc. Natl. Acad. Sci. USA* **114**, E6566-E6575. doi:10.1073/pnas.1701129114

Hanna, J., Goldman-Wohl, D., Hamani, Y., Avraham, I., Greenfield, C., Natanson-Yaron, S., Prus, D., Cohen-Daniel, L., Arnon, T. I., Manaster, I. et al. (2006). Decidual NK cells regulate key developmental processes at the human fetal-maternal interface. *Nat. Med.* **12**, 1065-1074. doi:10.1038/nm1452

Harris, L. K., Keogh, R. J., Wareing, M., Baker, P. N., Cartwright, J. E., Aplin, J. D. and Whitley, G. S. J. (2006). Invasive trophoblasts stimulate vascular smooth muscle cell apoptosis by a fas ligand-dependent mechanism. *Am. J. Pathol.* **169**, 1863-1874. doi:10.2353/ajpath.2006.060265

Hemberger, M. (2013). Immune balance at the foeto-maternal interface as the fulcrum of reproductive success. *J. Reprod. Immunol.* **97**, 36-42. doi:10.1016/j.jri.2012.10.006

Hess, A. P., Hamilton, A. E., Talbi, S., Dosiou, C., Nyegaard, M., Nayak, N., Genbecev-Krtolica, O., Mavrogianis, P., Ferrer, K., Kruessel, J. et al. (2007). Decidual stromal cell response to paracrine signals from the trophoblast: amplification of immune and angiogenic modulators. *Biol. Reprod.* **76**, 102-117. doi:10.1095/biolreprod.106.054791

Hoeltzenbein, M., Beck, E., Rajwanshi, R., Gøtestam Skorpen, C., Berber, E., Schaefer, C. and Østensen, M. (2016). Tocilizumab use in pregnancy: Analysis of a global safety database including data from clinical trials and post-marketing data. *Semin. Arthritis Rheum.* **46**, 238-245. doi:10.1016/j.semarthrit.2016.05.004

Hohensinner, P. J., Kaun, C., Rychli, K., Niessner, A., Pfaffenberger, S., Rega, G., de Martin, R., Maurer, G., Ullrich, R., Huber, K. et al. (2007). Macrophage colony stimulating factor expression in human cardiac cells is upregulated by tumor necrosis factor-alpha via an NF-kappaB dependent mechanism. *J. Thromb. Haemost.* **5**, 2520-2528. doi:10.1111/j.1538-7836.2007.02784.x

Hollister, A., Okubara, P., Watson, J. G. and Chaykin, S. (1987). Reproduction in mice: liver enlargement in mice during pregnancy and lactation. *Life Sci.* **40**, 11-18. doi:10.1016/0024-3205(87)90246-3

Hoshino, A., Costa-Silva, B., Shen, T.-L., Rodrigues, G., Hashimoto, A., Tesic Mark, M., Molina, H., Kohsaka, S., Di Giannatale, A., Ceder, S. et al. (2015). Tumour exosome integrins determine organotropic metastasis. *Nature* **527**, 329-335. doi:10.1038/nature15756

Houshdaran, S., Zelenko, Z., Irwin, J. C. and Giudice, L. C. (2014). Human endometrial DNA methylome is cycle-dependent and is associated with gene expression regulation. *Mol. Endocrinol.* **28**, 1118-1135. doi:10.1210/me.2013-1340

Huang, Z. and Feng, Y. (2017). Exosomes derived from hypoxic colorectal cancer cells promote angiogenesis through Wnt4-induced beta-catenin signaling in endothelial cells. *Oncol. Res.* **25**, 651-661. doi:10.3727/096504016X14752792816791

Huang, D. W., Sherman, B. T., Tan, Q., Collins, J. R., Alvord, W. G., Roayaei, J., Stephens, R., Baseler, M. W., Lane, H. C. and Lempicki, R. A. (2007). The DAVID Gene Functional Classification Tool: a novel biological module-centric algorithm to functionally analyze large gene lists. *Genome Biol.* **8**, R183. doi:10.1186/gb-2007-8-9-r183

Hunkapiller, N. M. and Fisher, S. J. (2008). Chapter 12 Placental remodeling of the uterine vasculature. *Methods Enzymol.* **445**, 281-302. doi:10.1016/S0076-6879(08)03012-7

Hytten, F. (1985). Blood volume changes in normal pregnancy. *Clin. Haematol.* **14**, 601-612.

Irwin, J. C., Kirk, D., King, R. J. B., Quigley, M. M. and Gwatkin, R. B. L. (1989). Hormonal regulation of human endometrial stromal cells in culture: an in vitro model for decidualization. *Fertil. Steril.* **52**, 761-768. doi:10.1016/S0015-0282(16)61028-2

Jeppesen, D. K., Fenix, A. M., Franklin, J. L., Higginbotham, J. N., Zhang, Q., Zimmerman, L. J., Liebler, D. C., Ping, J., Liu, Q., Evans, R. et al. (2019). Reassessment of exosome composition. *Cell* **177**, 428-445.e418. doi:10.1016/j.cell.2019.02.029

Johansen, C. B., Jimenez-Solem, E., Haerskjold, A., Sand, F. L. and Thomsen, S. F. (2018). The use and safety of TNF inhibitors during pregnancy in women with psoriasis: a review. *Int. J. Mol. Sci.* **19**, 1349. doi:10.3390/ijms19051349

Kalluri, R. and LeBleu, V. S. (2020). The biology, function, and biomedical applications of exosomes. *Science* **367**, eaau6977. doi:10.1126/science.aau6977

Kandzija, N., Zhang, W., Motta-Mejia, C., Mhlomi, V., McGowan-Downey, J., James, T., Cerdeira, A. S., Tannetta, D., Sargent, I., Redman, C. W. et al. (2019). Placental extracellular vesicles express active dipeptidyl peptidase IV; levels are increased in gestational diabetes mellitus. *J. Extracell. Vesicles* **8**, 1617000. doi:10.1080/20013078.2019.1617000

Kang, H.-B., Kim, Y.-E., Kwon, H.-J., Sok, D.-E. and Lee, Y. (2007). Enhancement of NF-kappaB expression and activity upon differentiation of human embryonic stem cell line SNUhES3. *Stem Cells Dev.* **16**, 615-623. doi:10.1089/scd.2007.0014

Knight, M., Redman, C. W. G., Linton, E. A. and Sargent, I. L. (1998). Shedding of syncytiotrophoblast microvilli into the maternal circulation in pre-eclamptic pregnancies. *Br. J. Obstet. Gynaecol.* **105**, 632-640. doi:10.1111/j.1471-0528.1998.tb10178.x

Kovats, S., Main, E. K., Librach, C., Stubblebine, M., Fisher, S. J. and DeMars, R. (1990). A class I antigen, HLA-G, expressed in human trophoblasts. *Science* **248**, 220-223. doi:10.1126/science.2326636

Kunsch, C. and Rosen, C. A. (1993). NF-kappa B subunit-specific regulation of the interleukin-8 promoter. *Mol. Cell. Biol.* **13**, 6137-6146. doi:10.1128/MCB.13.10.6137

Kuroki, K., Matsubara, H., Kanda, R., Miyashita, N., Shiroishi, M., Fukunaga, Y., Kamishikiryo, J., Fukunaga, A., Fukuhara, H., Hirose, K. et al. (2019). Structural and functional basis for LILRB immune checkpoint receptor recognition of HLA-G isoforms. *J. Immunol.* **203**, 3386-3394. doi:10.4049/jimmunol.1900562

Lain, K. Y. and Catalano, P. M. (2007). Metabolic changes in pregnancy. *Clin. Obstet. Gynecol.* **50**, 938-948. doi:10.1097/GRF.0b013e31815a5494

Libermann, T. A. and Baltimore, D. (1990). Activation of interleukin-6 gene expression through the NF-kappa B transcription factor. *Mol. Cell. Biol.* **10**, 2327-2334. doi:10.1128/MCB.10.5.2327

Lok, C. A. R., Van Der Post, J. A. M., Sargent, I. L., Hau, C. M., Sturk, A., Boer, K. and Nieuwland, R. (2008). Changes in microparticle numbers and cellular origin during pregnancy and preeclampsia. *Hypertens. Pregnancy* **27**, 344-360. doi:10.1080/10641950801955733

Lokossou, A. G., Toudic, C., Nguyen, P. T., Elisseeff, X., Vargas, A., Rassart, É., Lafond, J., Leduc, L., Bourgault, S., Gilbert, C. et al. (2019). Endogenous retrovirus-encoded Syncytin-2 contributes to exosome-mediated immunosuppression of T cells. *Biol. Reprod.* **102**, 185-198. doi:10.1093/biolre/ioz124

Lombardi, L., Ciana, P., Cappellini, C., Trecca, D., Guerrini, L., Migliazza, A., Maiolo, A. T. and Neri, A. (1995). Structural and functional characterization of the promoter regions of the NFKB2 gene. *Nucleic Acids Res.* **23**, 2328-2336. doi:10.1093/nar/23.12.2328

Lu, B., Rutledge, B. J., Gu, L., Fiorillo, J., Lukacs, N. W., Kunkel, S. L., North, R., Gerard, C. and Rollins, B. J. (1998). Abnormalities in monocyte recruitment and cytokine expression in monocyte chemoattractant protein 1-deficient mice. *J. Exp. Med.* **187**, 601-608. doi:10.1084/jem.187.4.601

Lynch, S., Santos, S. G., Campbell, E. C., Nimmo, A. M. S., Botting, C., Prescott, A., Antoniou, A. N. and Powis, S. J. (2009). Novel MHC class I structures on exosomes. *J. Immunol.* **183**, 1884-1891. doi:10.4049/jimmunol.0900798

Maltepe, E. and Fisher, S. J. (2015). Placenta: the forgotten organ. *Annu. Rev. Cell Dev. Biol.* **31**, 523-552. doi:10.1146/annurev-cellbio-100814-125620

Marino, M. W., Dunn, A., Grail, D., Inglese, M., Noguchi, Y., Richards, E., Jungbluth, A., Wada, H., Moore, M., Williamson, B. et al. (1997). Characterization of tumor necrosis factor-deficient mice. *Proc. Natl. Acad. Sci. USA* **94**, 8093-8098. doi:10.1073/pnas.94.15.8093

Matsushima, K., Larsen, C. G., DuBois, G. C. and Oppenheim, J. J. (1989). Purification and characterization of a novel monocyte chemotactic and activating factor produced by a human myelomonocytic cell line. *J. Exp. Med.* **169**, 1485-1490. doi:10.1084/jem.169.4.1485

McMaster, M. T., Librach, C. L., Zhou, Y., Lim, K. H., Janatpour, M. J., DeMars, R., Kovats, S., Damsky, C. and Fisher, S. J. (1995). Human placental HLA-G expression is restricted to differentiated cytotrophoblasts. *J. Immunol.* **154**, 3771-3778.

McMaster, M., Zhou, Y., Shorter, S., Kapasi, K., Geraghty, D., Lim, K. H. and Fisher, S. (1998). HLA-G isoforms produced by placental cytotrophoblasts and found in amniotic fluid are due to unusual glycosylation. *J. Immunol.* **160**, 5922-5928.

Medina, J. and Workman, J. L. (2018). Maternal experience and adult neurogenesis in mammals: Implications for maternal care, cognition, and mental health. *J. Neurosci. Res.* **98**, 1293-1308. doi:10.1002/jnr.24311

Motta-Mejia, C., Kandzija, N., Zhang, W., Mhlomi, V., Cerdeira, A. S., Burdujan, A., Tannetta, D., Dragovic, R., Sargent, I. L., Redman, C. W. et al. (2017). Placental vesicles carry active endothelial nitric oxide synthase and their activity is reduced in preeclampsia. *Hypertension* **70**, 372-381. doi:10.1161/HYPERTENSIONAHA.117.09321

Nakamura, H., Kimura, T., Ogita, K., Koyama, S., Tsujie, T., Tsutsui, T., Shimoya, K., Koyama, M., Kaneda, Y. and Murata, Y. (2004). Alteration of the timing of implantation by in vivo gene transfer: delay of implantation by suppression of nuclear factor kappaB activity and partial rescue by leukemia inhibitory factor. *Biochem. Biophys. Res. Commun.* **321**, 886-892. doi:10.1016/j.bbrc.2004.07.045

Osmers, R. G., Blaser, J., Kuhn, W. and Tschesche, H. (1995). Interleukin-8 synthesis and the onset of labor. *Obstet. Gynecol.* **86**, 223-229. doi:10.1016/0029-7844(95)93704-4

Ouyang, Y., Bayer, A., Chu, T., Tyurin, V. A., Kagan, V. E., Morelli, A. E., Coyne, C. B. and Sadovsky, Y. (2016). Isolation of human trophoblastic extracellular vesicles and characterization of their cargo and antiviral activity. *Placenta* **47**, 86-95. doi:10.1016/j.placenta.2016.09.008

Pascolo, S., Ginhoux, F., Laham, N., Walter, S., Schoor, O., Probst, J., Rohrlich, P., Obermayr, F., Fisch, P., Danos, O. et al. (2005). The non-classical HLA class I molecule HFE does not influence the NK-like activity contained in fresh human PBMCs and does not interact with NK cells. *Int. Immunol.* **17**, 117-122. doi:10.1093/intimm/dxh191

Pasparakis, M., Alexopoulou, L., Episkopou, V. and Kollias, G. (1996). Immune and inflammatory responses in TNF alpha-deficient mice: a critical requirement for TNF alpha in the formation of primary B cell follicles, follicular dendritic cell networks and germinal centers, and in the maturation of the humoral immune response. *J. Exp. Med.* **184**, 1397-1411. doi:10.1084/jem.184.4.1397

Peinado, H., Alečković, M., Lavotshkin, S., Matei, I., Costa-Silva, B., Moreno-Bueno, G., Hergueta-Redondo, M., Williams, C., García-Santos, G., Ghajar, C. et al. (2012). Melanoma exosomes educate bone marrow progenitor cells toward a pro-metastatic phenotype through MET. *Nat. Med.* **18**, 883-891. doi:10.1038/nm.2753

Phillips, T. A., Ni, J. and Hunt, J. S. (2001). Death-inducing tumour necrosis factor (TNF) superfamily ligands and receptors are transcribed in human placentae, cytotrophoblasts, placental macrophages and placental cell lines. *Placenta* **22**, 663-672. doi:10.1053/plac.2001.0703

Pijnenborg, R., McLaughlin, P. J., Vercruysse, L., Hanssens, M., Johnson, P. M., Keith, J. C., Jr and Van Assche, F. A. (1998). Immunolocalization of tumour necrosis factor-α (TNF-α) in the placental bed of normotensive and hypertensive human pregnancies. *Placenta* **19**, 231-239. doi:10.1016/S0143-4004(98)90054-6

Poggio, M., Hu, T., Pai, C.-C., Chu, B., Belair, C. D., Chang, A., Montabana, E., Lang, U. E., Fu, Q., Fong, L. et al. (2019). Suppression of Exosomal PD-L1 Induces Systemic Anti-tumor Immunity and Memory. *Cell* **177**, 414-427.e413. doi:10.1016/j.cell.2019.02.016

Raposo, G. and Stoorvogel, W. (2013). Extracellular vesicles: exosomes, microvesicles, and friends. *J. Cell Biol.* **200**, 373-383. doi:10.1083/jcb.201211138

Red-Horse, K., Drake, P. M., Gunn, M. D. and Fisher, S. J. (2001). Chemokine ligand and receptor expression in the pregnant uterus: reciprocal patterns in complementary cell subsets suggest functional roles. *Am. J. Pathol.* **159**, 2199-2213. doi:10.1016/S0002-9440(10)63071-4

Red-Horse, K., Kapidzic, M., Zhou, Y., Feng, K.-T., Singh, H. and Fisher, S. J. (2005). EPHB4 regulates chemokine-evoked trophoblast responses: a mechanism for incorporating the human placenta into the maternal circulation. *Development* **132**, 4097-4106. doi:10.1242/dev.01971

Red-Horse, K., Rivera, J., Schanz, A., Zhou, Y., Winn, V., Kapidzic, M., Maltepe, E., Okazaki, K., Kochman, R., Vo, K. C. et al. (2006). Cytotrophoblast induction of arterial apoptosis and lymphangiogenesis in an in vivo model of human placentation. *J. Clin. Invest.* **116**, 2643-2652. doi:10.1172/JCI27306.

Rinaldi, S. F., Makieva, S., Saunders, P. T., Rossi, A. G. and Norman, J. E. (2017). Immune cell and transcriptomic analysis of the human decidua in term and preterm parturition. *Mol. Hum. Reprod.* **23**, 708-724. doi:10.1093/molehr/gax038

Rivoltini, L., Chiodoni, C., Squarcina, P., Tortoreto, M., Villa, A., Vergani, B., Bürdek, M., Botti, L., Arioli, I., Cova, A. et al. (2016). TNF-Related Apoptosis-Inducing Ligand (TRAIL)-armed exosomes deliver proapoptotic signals to tumor site. *Clin. Cancer Res.* **22**, 3499-3512. doi:10.1158/1078-0432.CCR-15-2170

Robertson, S. A., Christiaens, I., Dorian, C. L., Zaragoza, D. B., Care, A. S., Banks, A. M. and Olson, D. M. (2010). Interleukin-6 is an essential determinant of on-time parturition in the mouse. *Endocrinology* **151**, 3996-4006. doi:10.1210/en.2010-0063

Robinson, J. F., Kapidzic, M., Gormley, M., Ona, K., Dent, T., Seifikar, H., Hamilton, E. G. and Fisher, S. J. (2017). Transcriptional dynamics of cultured human villous cytotrophoblasts. *Endocrinology* **158**, 1581-1594. doi:10.1210/en.2016-1635

Rosenberger, G., Koh, C. C., Guo, T., Röst, H. L., Kouvonen, P., Collins, B. C., Heusel, M., Liu, Y., Caron, E., Vichalkovski, A. et al. (2014). A repository of assays to quantify 10,000 human proteins by SWATH-MS. *Sci. Data* **1**, 140031. doi:10.1038/sdata.2014.31

Saji, F., Samejima, Y., Kamiura, S. and Koyama, M. (1999). Dynamics of immunoglobulins at the feto-maternal interface. *Rev. Reprod.* **4**, 81-89. doi:10.1530/ror.0.0040081

Sakamoto, Y., Moran, P., Searle, R. F., Bulmer, J. N. and Robson, S. C. (2004). Interleukin-8 is involved in cervical dilatation but not in prelabour cervical ripening. *Clin. Exp. Immunol.* **138**, 151-157. doi:10.1111/j.1365-2249.2004.02584.x

Salomon, C., Torres, M. J., Kobayashi, M., Scholz-Romero, K., Sobrevia, L., Dobierzewska, A., Illanes, S. E., Mitchell, M. D. and Rice, G. E. (2014). A gestational profile of placental exosomes in maternal plasma and their effects on endothelial cell migration. *PLoS ONE* **9**, e98667. doi:10.1371/journal.pone.0098667

Sarker, S., Scholz-Romero, K., Perez, A., Illanes, S. E., Mitchell, M. D., Rice, G. E. and Salomon, C. (2014). Placenta-derived exosomes continuously increase in maternal circulation over the first trimester of pregnancy. *J. Transl. Med.* **12**, 204. doi:10.1186/1479-5876-12-204

Savina, A., Vidal, M. and Colombo, M. I. (2002). The exosome pathway in K562 cells is regulated by Rab11. *J. Cell Sci.* **115**, 2505-2515.

Schilling, B., Christensen, D., Davis, R., Sahu, A. K., Hu, L. I., Walker-Peddakotla, A., Sorensen, D. J., Zemaitaitis, B., Gibson, B. W. and Wolfe, A. J. (2015). Protein acetylation dynamics in response to carbon overflow in Escherichia coli. *Mol. Microbiol.* **98**, 847-863. doi:10.1111/mmi.13161

Schilling, B., Gibson, B. W. and Hunter, C. L. (2017). Generation of High-Quality SWATH((R)) acquisition data for label-free quantitative proteomics studies using TripleTOF((R)) mass spectrometers. *Methods Mol. Biol.* **1550**, 223-233. doi:10.1007/978-1-4939-6747-6_16

Shankar, J., Messenberg, A., Chan, J., Underhill, T. M., Foster, L. J. and Nabi, I. R. (2010). Pseudopodial actin dynamics control epithelial-mesenchymal transition in metastatic cancer cells. *Cancer Res.* **70**, 3780-3790. doi:10.1158/0008-5472.CAN-09-4439

Shingo, T., Gregg, C., Enwere, E., Fujikawa, H., Hassam, R., Geary, C., Cross, J. C. and Weiss, S. (2003). Pregnancy-stimulated neurogenesis in the adult female forebrain mediated by prolactin. *Science* **299**, 117-120. doi:10.1126/science.1076647

Shiroishi, M., Kuroki, K., Ose, T., Rasubala, L., Shiratori, I., Arase, H., Tsumoto, K., Kumagai, I., Kohda, D. and Maenaka, K. (2006). Efficient leukocyte Ig-like receptor signaling and crystal structure of disulfide-linked HLA-G dimer. *J. Biol. Chem.* **281**, 10439-10447. doi:10.1074/jbc.M512305200

Silva, T. A., Smuczek, B., Valadão, I. C., Dzik, L. M., Iglesia, R. P., Cruz, M. C., Zelanis, A., de Siqueira, A. S., Serrano, S. M. T., Goldberg, G. S. et al. (2016). AHNAK enables mammary carcinoma cells to produce extracellular vesicles that increase neighboring fibroblast cell motility. *Oncotarget* **7**, 49998-50016. doi:10.18632/oncotarget.10307

Simister, N. E. and Mostov, K. E. (1989). An Fc receptor structurally related to MHC class I antigens. *Nature* **337**, 184-187. doi:10.1038/337184a0

Simister, N. E., Story, C. M., Chen, H.-L. and Hunt, J. S. (1996). An IgG-transporting Fc receptor expressed in the syncytiotrophoblast of human placenta. *Eur. J. Immunol.* **26**, 1527-1531. doi:10.1002/eji.1830260718

Smith, C. H., Nelson, D. M., King, B. F., Donohue, T. M., Ruzycki, S. and Kelley, L. K. (1977). Characterization of a microvillous membrane preparation from human placental syncytiotrophoblast: a morphologic, biochemical, and physiologic, study. *Am. J. Obstet. Gynecol.* **128**, 190-196. doi:10.1016/0002-9378(77)90686-X

Son, Y.-H., Jeong, Y.-T., Lee, K.-A., Choi, K.-H., Kim, S.-M., Rhim, B.-Y. and Kim, K. (2008). Roles of MAPK and NF-kappaB in interleukin-6 induction by lipopolysaccharide in vascular smooth muscle cells. *J. Cardiovasc. Pharmacol.* **51**, 71-77. doi:10.1097/FJC.0b013e31815bd23d

Tannetta, D. S., Dragovic, R. A., Gardiner, C., Redman, C. W. and Sargent, I. L. (2013). Characterisation of syncytiotrophoblast vesicles in normal pregnancy and pre-eclampsia: expression of Flt-1 and endoglin. *PLoS ONE* **8**, e56754. doi:10.1371/journal.pone.0056754

Tannetta, D. S., Hunt, K., Jones, C. I., Davidson, N., Coxon, C. H., Ferguson, D., Redman, C. W., Gibbins, J. M., Sargent, I. L. and Tucker, K. L. (2015). Syncytiotrophoblast extracellular vesicles from pre-eclampsia placentas differentially affect platelet function. *PLoS ONE* **10**, e0142538. doi:10.1371/journal.pone.0142538

Tannetta, D., Collett, G., Vatish, M., Redman, C. and Sargent, I. (2017). Syncytiotrophoblast extracellular vesicles - circulating biopsies reflecting placental health. *Placenta* **52**, 134-138. doi:10.1016/j.placenta.2016.11.008

Ten, R. M., Paya, C. V., Israël, N., Le Bail, O., Mattei, M. G., Virelizier, J. L., Kourilsky, P. and Israël, A. (1992). The characterization of the promoter of the gene encoding the p50 subunit of NF-kappa B indicates that it participates in its own regulation. *EMBO J.* **11**, 195-203. doi:10.1002/j.1460-2075.1992.tb05042.x

Théry, C., Amigorena, S., Raposo, G. and Clayton, A. (2006). Isolation and characterization of exosomes from cell culture supernatants and biological fluids. *Curr. Protoc. Cell Biol.* **30**, 3.22.1-3.22.29. doi:10.1002/0471143030.cb0322s30

Ueda, A., Okuda, K., Ohno, S., Shirai, A., Igarashi, T., Matsunaga, K., Fukushima, J., Kawamoto, S., Ishigatsubo, Y. and Okubo, T. (1994). NF-kappa B and Sp1 regulate transcription of the human monocyte chemoattractant protein-1 gene. *J. Immunol.* **153**, 2052-2063.

Valente, A. J., Graves, D. T., Vialle-Valentin, C. E., Delgado, R. and Schwartz, C. J. (1988). Purification of a monocyte chemotactic factor secreted by nonhuman

primate vascular cells in culture. *Biochemistry* **27**, 4162-4168. doi:10.1021/bi00411a039

van de Stolpe, A., Caldenhoven, E., Stade, B. G., Koenderman, L., Raaijmakers, J. A., Johnson, J. P. and van der Saag, P. T. (1994). 12-O-tetradecanoylphorbol-13-acetate- and tumor necrosis factor alpha-mediated induction of intercellular adhesion molecule-1 is inhibited by dexamethasone. Functional analysis of the human intercellular adhesion molecular-1 promoter. *J. Biol. Chem.* **269**, 6185-6192.

van de Vlekkert, D., Demmers, J., Nguyen, X.-X., Campos, Y., Machado, E., Annunziata, I., Hu, H., Gomero, E., Qiu, X., Bongiovanni, A. et al. (2019). Excessive exosome release is the pathogenic pathway linking a lysosomal deficiency to generalized fibrosis. *Sci. Adv.* **5**, eaav3270. doi:10.1126/sciadv.aav3270

Vigneron, N., Ferrari, V., Stroobant, V., Abi Habib, J. and Van den Eynde, B. J. (2017). Peptide splicing by the proteasome. *J. Biol. Chem.* **292**, 21170-21179. doi:10.1074/jbc.R117.807560

Wagenblast, E., Soto, M., Gutiérrez-Ángel, S., Hartl, C. A., Gable, A. L., Maceli, A. R., Erard, N., Williams, A. M., Kim, S. Y., Dickopf, S. et al. (2015). A model of breast cancer heterogeneity reveals vascular mimicry as a driver of metastasis. *Nature* **520**, 358-362. doi:10.1038/nature14403

Yelavarthi, K. K., Fishback, J. L. and Hunt, J. S. (1991). Analysis of HLA-G mRNA in human placental and extraplacental membrane cells by in situ hybridization. *J. Immunol.* **146**, 2847-2854.

Zhang, H.-G., Liu, C., Su, K., Yu, S., Zhang, L., Zhang, S., Wang, J., Cao, X., Grizzle, W. and Kimberly, R. P. (2006). A membrane form of TNF-α presented by exosomes delays T cell activation-induced cell death. *J. Immunol.* **176**, 7385-7393. doi:10.4049/jimmunol.176.12.7385

Zhou, A., Scoggin, S., Gaynor, R. B. and Williams, N. S. (2003). Identification of NF-kappa B-regulated genes induced by TNFα utilizing expression profiling and RNA interference. *Oncogene* **22**, 2054-2064. doi:10.1038/sj.onc.1206262

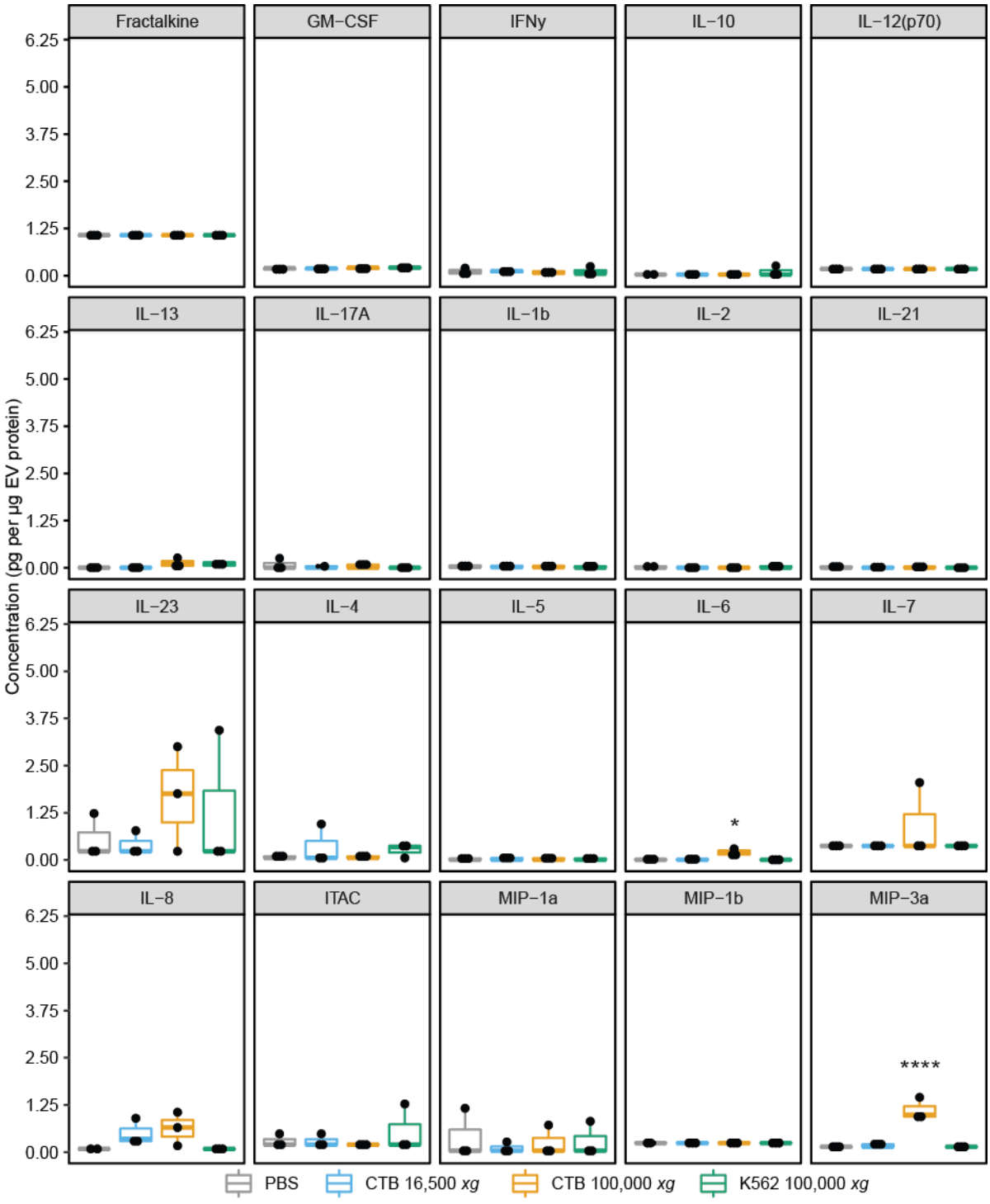

Fig. S1. Cytotrophoblast (CTB) extracellular vesicles (EVs) lacked detectable levels of most analytes measured by cytokine array. EVs (2 µg protein) were analyzed by a high sensitivity cytokine array. Most analytes were below the threshold of detection. In the CTB 100,000 *xg* pellet, IL-6 was present at ~0.2 pg/µg and MIP-3a was detected at ~1 pg/µg. n=3 biological replicates. * p<0.05, **** p<0.001.

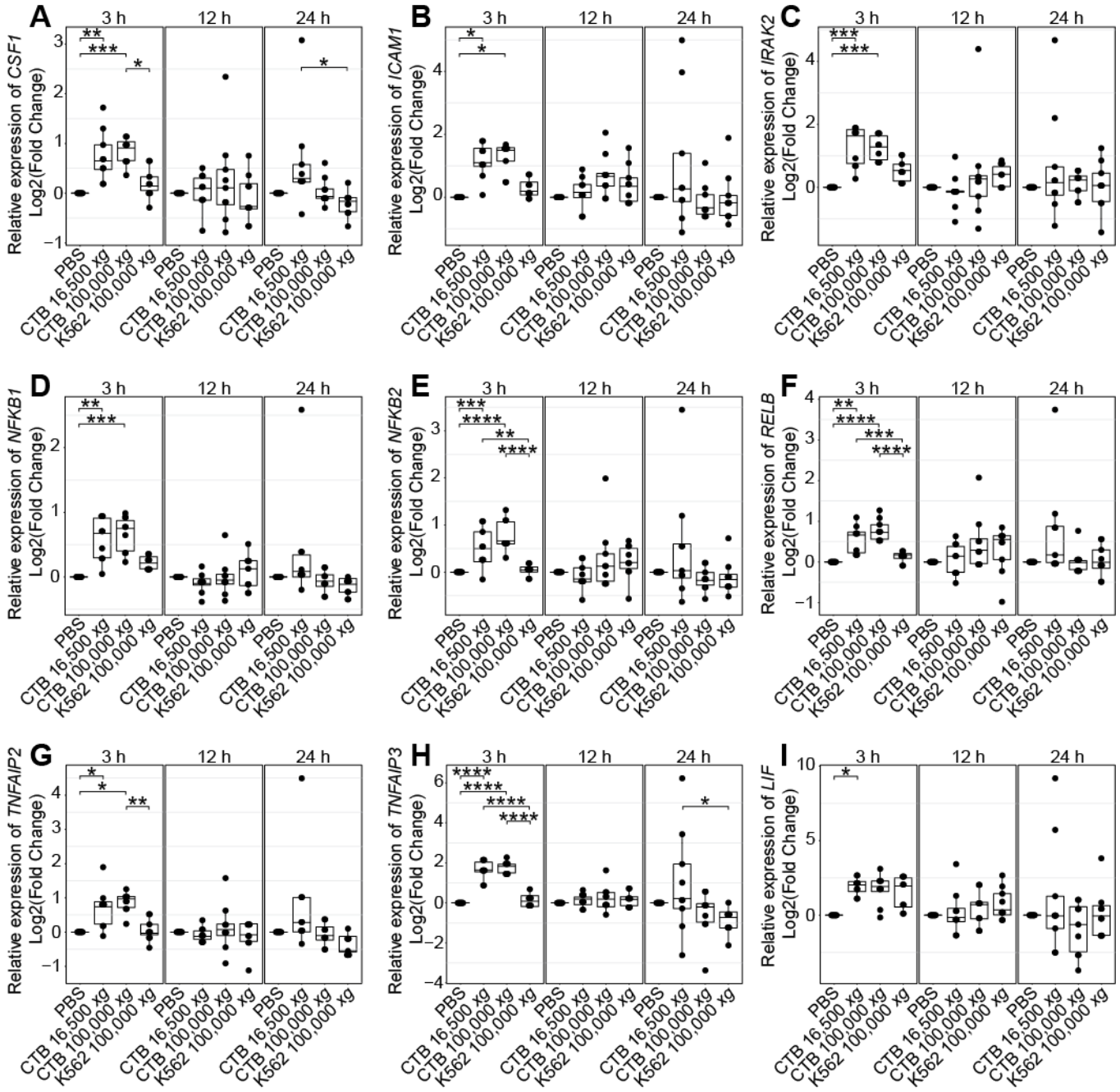

Fig. S2. Quantification of cytotrophoblast (CTB) extracellular vesicle (EV) effects on decidualized endometrial stromal fibroblast (dESF) expression of mRNAs encoding additional NF-κB targets. Data augment that shown in Fig. 6. n=3 biological replicates (EV batches and dESFs). * p<0.05, ** p<0.01, *** p<0.005, **** p<0.001.

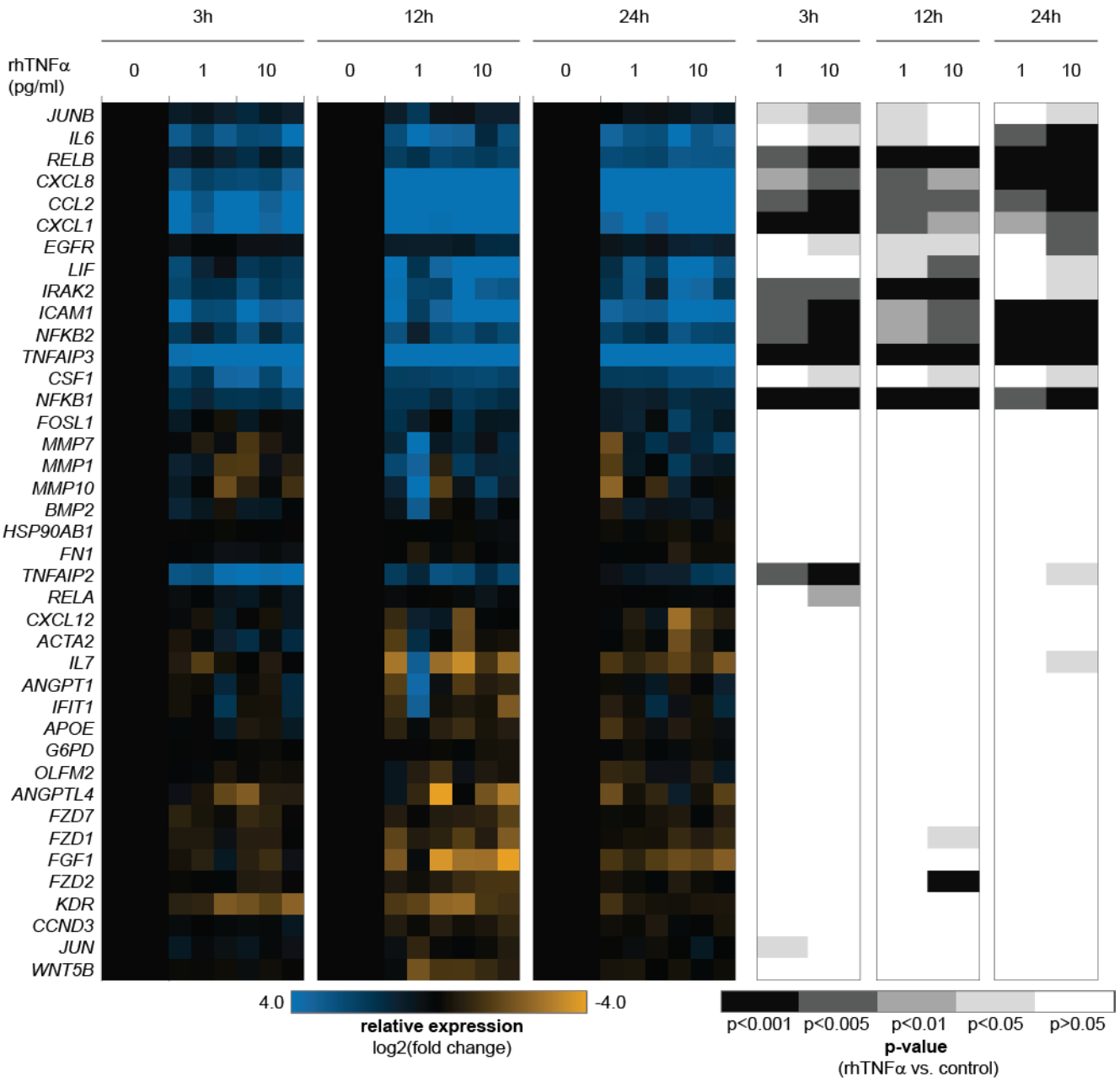

Fig. S3. Recombinant human TNF-α (rhTNF-α) sustained increased decidualized endometrial stromal fibroblast (dESF) expression of the mRNAs encoding NF-κB targets for the duration of the 24 h time course. Heat maps of gene expression changes (left) and p-values (right) compared to the PBS control. dESFs were treated with rhTNF-α and high throughput qRT-PCR was performed using a Fluidigm 96.96 Dynamic Array IFC. Enhanced transcription of NF-κB targets was sustained over the course of the experiment. n=3 biological replicates (dESFs).

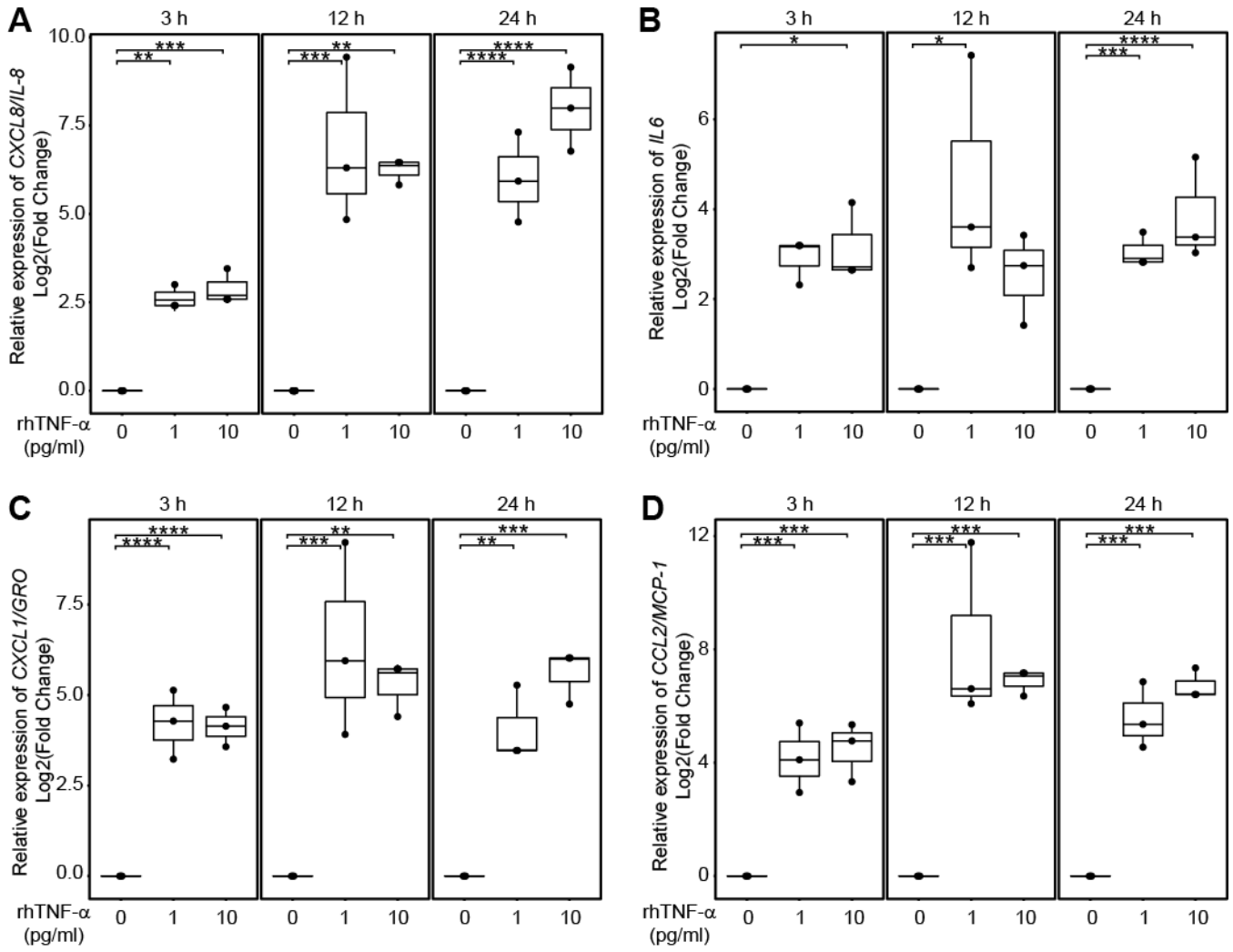

Fig. S4. rhTNF-α increased decidualized endometrial stromal fibroblast (dESF) expression of mRNAs encoding *CXCL8/IL-8, IL-6, CXCL1/GRO*, and *CCL2/MCP-1* for the duration of the 24 h time course. Changes in gene expression were measured with a Fluidigm 96.96 Dynamic Array IFC. The addition of rhTNF-α (1 or 10 pg/ml) increased transcription of (A) *CXCL8/IL-8*, (B) *IL-6*, (C) *CXCL1/GRO*, and (D) *CCL2/MCP-1* at the time points indicated. n=3 biological replicates (dESFs). * p<0.05, ** p<0.01, *** p<0.005, **** p<0.001.

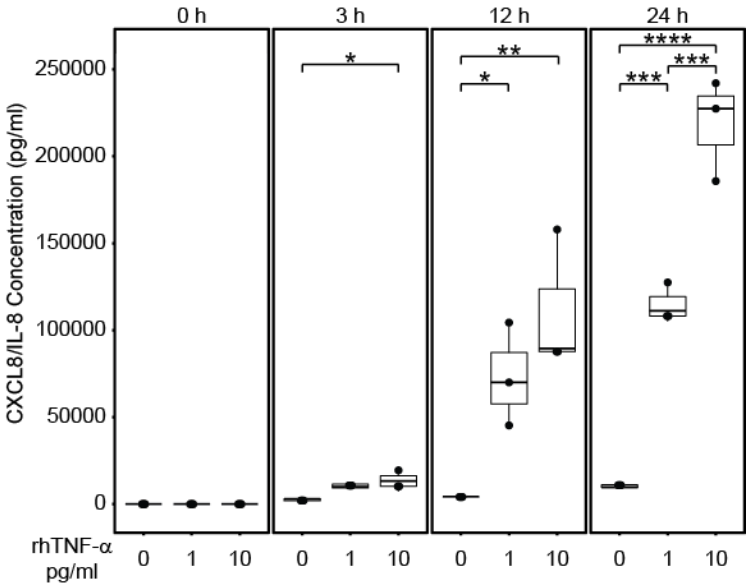

Fig. S5. Recombinant human TNF-α (rhTNF-α) increased decidualized endometrial stromal fibroblast (dESF) IL-8 secretion. Over the course of the experiment (24 h), rhTNF-α treatment (1 or 10 pg/ml) induced dESF secretion of IL-8 in a concentration dependent manner as measured by ELISA. n=3 biological replicates (dESFs). * $p<0.05$, ** $p<0.01$, *** $p<0.005$, **** $p<0.001$.

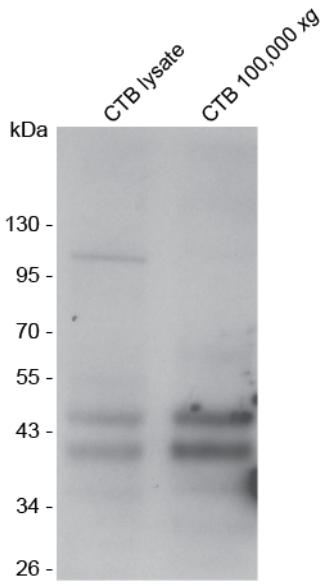

Fig. S6. Immunoblot analysis showed that cytotrophoblast (CTB) lysate and the 100,000 *xg* fraction contained proteins of the expected molecular weight that reacted with anti-neonatal Fc receptor (FcRn). n=1.

Table S1. 16,500xg Extracellular Vesicle Fraction

Click here to Download Table S1

Table S2. 100,000xg Extracellular Vesicle Fraction

Click here to Download Table S2

Table S3. Antibodies for immunoblotting and immunofluorescence

Primary Antibodies						Secondary Antibodies			
Target	**Clone**	**Supplier**	**Catalog #**	**Host**	**Dilution**	**Antibody**	**Conjugate**	**Supplier**	**Dilution**
CD9	KMC8	BD Biosciences	BDB553758	rat	1:250	Donkey anti-rat	Peroxidase	Jackson ImmunoResearch Labs, Inc.	1:5000
CK	7D3	Laboratory of S.J. Fisher	N/A	rat	1:100	Donkey anti-rat	Rhodamine	Jackson ImmunoResearch Labs, Inc.	1:100
FN	Clone 10/ Fibronectin	BD Biosciences	610077	mouse	1:1000	Donkey anti-mouse	Peroxidase	Jackson ImmunoResearch Labs, Inc.	1:5000
FcRn	Polyclonal	Laboratory of N.E. Simister	N/A	mouse	1:200	Donkey anti-mouse	Peroxidase	Jackson ImmunoResearch Labs, Inc.	1:5000
HLA-G	4H84	Laboratory of S.J. Fisher	N/A	mouse	1:250	Donkey anti-mouse	Peroxidase	Jackson ImmunoResearch Labs, Inc.	1:5000
HRS	D7T5N	Cell Signaling Technology	15087	rabbit	1:1000	Donkey anti-rabbit	Peroxidase	Jackson ImmunoResearch Labs, Inc.	1:5000
PD-L1	E1L3N	Cell Signaling Technology	13684	rabbit	1:1000	Donkey anti-rabbit	Peroxidase	Jackson ImmunoResearch Labs, Inc.	1:5000
PLAP	EPR6141	Millipore Sigma	MABC644	rabbit	1:750	Donkey anti-rabbit	Peroxidase	Jackson ImmunoResearch Labs, Inc.	1:5000
TNF-α	2C8	Abcam	ab8348	mouse	1:100	Donkey anti-mouse	FITC	Jackson ImmunoResearch Labs, Inc.	1:100

Table S4. qRT-PCR primers

Target	Forward Primer	Reverse Primer
ACTA2	AAGGCCAACCGGGAGAAAA	CGCCTGGATAGCCACATACA
ANGPT1	TCCAAAGAGGCTGGAAGGAA	CCTCTGACTGGTAATGGCAAAA
ANGPTL4	TCCACTTGGGACCAGGATCA	AATGGCTGCAGGTGCCAAA
APOE	CCCAGGTCACCCAGGAAC	TGTTCCTCCAGTTCCGATTTGTA
BMP2	ACTGTGCGCAGCTTCCA	ACTCCTCCGTGGGGATAGAA
CCL2	TAGCAGCCACCTTCATTCCC	CCTCTGCACTGAGATCTTCCTA
CCND3	CGACAGGCCTTGGTCAAAA	ATCATGGATGGCGGGTACA
CSF1	GGAGACCTCGTGCCAAATTA	TGCCTTCTTAAGGTAGCACAC
CXCL1	CTTGCCTCAATCCTGCATCC	AGCCACCAGTGAGCTTCC
CXCL12	GCTGGTCCTCGTGCTGAC	GAATCGGCATGGGCATCTGTA
CXCL8	ACACTGCGCCAACACAGAAA	CAGTTTTCCTTGGGGTCCAGAC
EGFR	AGTGTAAGAAGTGCGAAGGG	TCGTAGCATTTATGGAGAGTGAG
FGF1	TCTGCCTCCAGGGAATTACA	CCTGTCCCTTGTCCCATCC
FN1	GTGTGTGTGTCTTGGTAATGGAAA	AGTCCCAGCAGCATGATCAA
FOSL1	ATTGAGGAGCTGCAGAAGCA	CCCTCCTTGGCTCCTTCC
FZD1	GCTTCGTGGGGCTTAACAAC	ACGTGCCGATAAACAGGTACA
FZD2	CCTTCTTCACTGTCACCACGTA	TGTAGCAGCCCGACAGAAAA
FZD7	TCCGCACCATCATGAAACAC	GTGTAGAGCACGCTGAAGAC
G6PD	GCCGTCACCAAGAACATTCA	CTCCCGAAGGGCTTCTCC
HSP90AB1	TCCTTCGGGAGTTGATCTCTA	GGGTCTGTCAGGCTCTCATA
ICAM1	CCCCTACCAGCTCCAGACC	TGCGTGTCCACCTCTAGGAC
IFIT1	AGGCTGTCCGCTTAAATCCA	TCAGCTTCCTGTCCTTCATCC
IL6	AGAGCTGTGCAGATGAGTACAA	GTTGGGTCAGGGGTGGTTA
IL7	ATTGAAGGTAAAGATGGCAAACA	TCATTATTCAGGCAATTGCTACC
IRAK2	GTCTGGAGATCATCCACAGCAA	TGAGCCATTGGGTGAGCAA
JUN	AAGAACTCGGACCTCCTCAC	TGGATTATCAGGCGCTCCA
JUNB	TGGCCCAGCTCAAACAGAA	AGAAGGCGTGTCCCTTGAC
KDR	AGTGGGCTGATGACCAAGAA	CCATGCCACTTCCAAAAGCA
LIF	CTCGGGTAAGGATGTCTTCCA	ACACGGCGATGATCTGCTTA
MMP1	CACCTTCAGTGGTGATGTTCA	GCTGGACAGGATTTTGGGAA
MMP10	TGAGCCTAAGGTTGATGCTGTA	GGCATTGGGGTCAAACTCAA
MMP7	TGTATGGGGAACTGCTGACA	ATGAGCCAGCGTGTTTCC
NFKB1	CTACCTGGTGCCTCTAGTGAAA	ACCTTTGCTGGTCCCACATA
NFKB2	TACCTGGTGATCGTGGAACA	GCCTTCACAGCCATATCGAA
OLFM2	GGCTCCTGGATGACTGACA	GGCGGCCTTTGTAATAGCC
RELA	GCATCCAGACCAACAACAACC	AGAGCCGCACAGCATTCA
RELB	TGCTTTCCGAGCCCGTCTA	CGGCCCGCTTTCCTTGTTAA
TNFAIP2	AAGAGCCACGGCTTTGACA	GTGTGCGTGAACCTCTTGAAC
TNFAIP3	GAAGCTTGTGGCGCTGAAAA	CCTGAACGCCCCACATGTA
WNT5B	ATTGCAGCACAGCGGACAA	CTCACCGCGTGGGTGAA